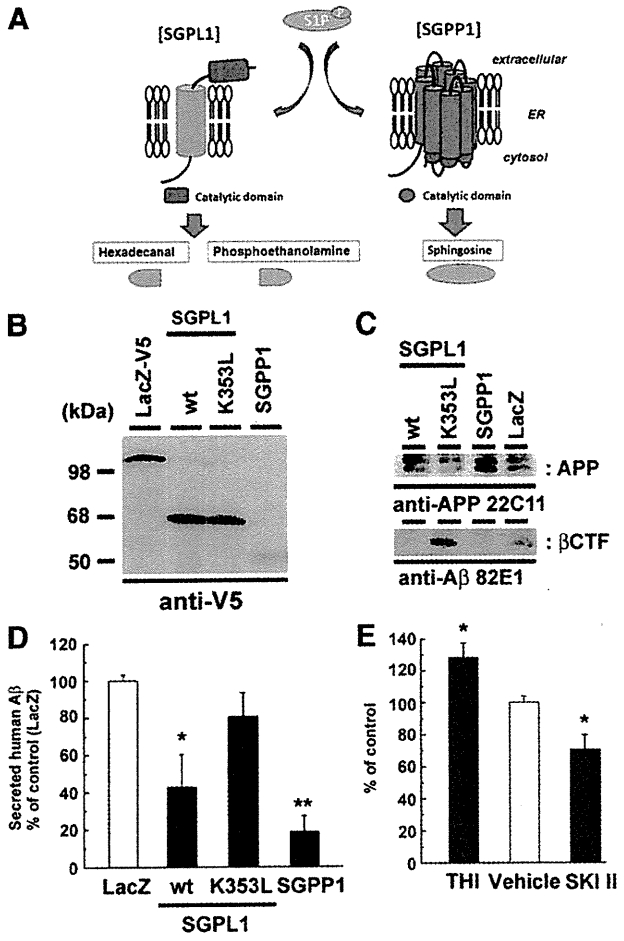

Figure 5. Effect of S1P degrading enzymes on Aβ production. ***A***, Schematic view of S1P degradation pathway. Note that SGPL1 and SGPP1 generate different degradation products of S1P. ER, Endoplasmic reticulum. ***B–D***, Effects of the overexpression of V5-tagged S1P degrading enzymes on APP metabolism in N2a cells. N2a cells were cotransfected with S1P degrading enzymes and Swedish mutant of APP. After 24 h transfection, media were replaced and further incubated for 24 h. Immunoblot analysis of S1P degrading enzymes (***B***) and APP derivatives (***C***) are shown. Human APP-derived βCTF was specifically detected by an anti-human Aβ N-terminus antibody (82E1). wt, Wild type. ***D***, The levels of secreted human Aβ was detected by human Aβ-specific ELISA ($n = 4$; mean ± SEM; $^*p < 0.05$, $^{**}p < 0.01$). Note that overexpression of SGPL1 or SGPP1, but not SGPL1 carrying catalytically inactive mutation (K353L), decreased the generation of βCTF and the Aβ secretion from N2a cells. ***E***, The levels of secreted Aβ from mouse primary cortical neurons (7 d *in vitro*) treated with SGPL1 inhibitor THI (50 μg/ml) or SKI II (1 μM) for 24 h ($n = 4$; mean ± SEM; $^*p < 0.05$).

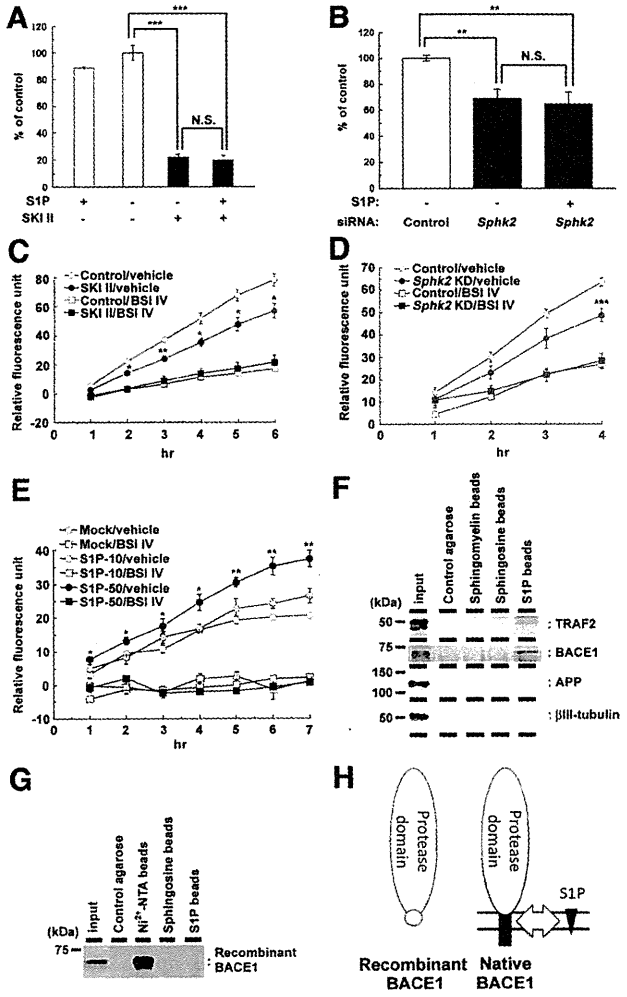

Figure 6. SKI II treatment decreased the β-secretase activity in cellular membrane. ***A***, ***B***, Effect of extracellularly added S1P (10 μM) on levels of secreted Aβ from mouse primary cortical neurons (7 d *in vitro*) after treatment with SKI II (1 μM) for 24 h (***A***) ($n = 4$; mean ± SEM) or from N2a cells after 48 h *SphK2* knockdown (***B***) ($n = 3$; mean ± SEM; $^{**}p < 0.01$, $^{***}p < 0.001$; N.S., no significant difference). Note that S1P failed to rescue the decrease in Aβ production either by SKI II or *SphK2* knockdown. ***C***, β-Secretase activity in the membrane fractions of N2a cells treated with vehicle or SKI II (1 μM) for 24 h. BACE inhibitor IV (BSI IV; 1 μM) was added to the *in vitro* assay ($n = 3$; mean ± SEM; $^*p < 0.05$, $^{**}p < 0.01$ vs control/vehicle). ***D***, β-Secretase activity in the membrane fractions of *SphK2* knockdown N2a cells. BACE inhibitor IV (BSI IV; 1 μM) was added to the *in vitro* assay ($n = 3$; mean ± SEM; $^{***}p < 0.001$ vs control/vehicle). ***E***, Effect of S1P on β-secretase activity in the membrane fractions of mouse brain. S1P (10 or 50 μM) and BACE inhibitor IV (BSI IV; 1 μM) were added to the *in vitro* assay ($n = 3$; mean ± SEM; $^*p < 0.05$, $^{**}p < 0.01$ vs mock/vehicle). ***F***, ***G***, Association of BACE1 holoprotein with immobilized S1P. N2a cell lysates (***F***) or recombinant BACE1 with 10×His tag that lacks the transmembrane and cytoplasmic domains (***G***) were incubated with control agarose (no lipid), Nickel-NTA agarose, sphingomyelin, sphingosine, or S1P-coated affinity matrices (as indicated), and bound proteins were analyzed by immunoblotting. ***H***, Schematic model of the binding of BACE1 and S1P. S1P (black triangles) interacts with the C-terminal region of BACE1 (black squares), including the transmembrane domain, but not with the extracellular protease domain (white ovals). Location of 10×His tag is indicated by a white circle.

TRAF2 to S1P beads as described recently (Alvarez et al., 2010). Furthermore, endogenous BACE1, but not APP, was specifically pulled down by matrices carrying S1P. In contrast, recombinant BACE1 protein that lacks the transmembrane and cytoplasmic domains was never bound to S1P beads (Fig. 6*G*). Collectively, these results strongly suggest that the cell-associated S1P modulates the proteolytic activity of membrane-bound form of BACE1 via direct interaction (Fig. 6*H*).

Roles of SphK2 activity in Alzheimer's disease

Data shown above indicate that the intracellular S1P is one of the important determinants for BACE1 activity. We further examined the impact of reduced S1P levels on Aβ levels *in vivo*. Stereotaxic injection of SKI II into wild-type mouse brain significantly decreased the amount of endogenous Aβ at hippocampus (Fig. 7*A*). Because SKI II exhibited a favorable bioavailability (French et al., 2006), we next orally administered SKI II to APP transgenic mice A7 overexpressing human APP carrying Swedish and Austrian mutations (Yamada et al., 2009). After 6 d treatment with SKI II in 6-month-old female mice, in which pathologically detectable amyloid plaques have not been developed, the total Aβ levels in brains were significantly decreased (Fig. 7*B*). These data indicate that the inhibition of SphK activity in APP

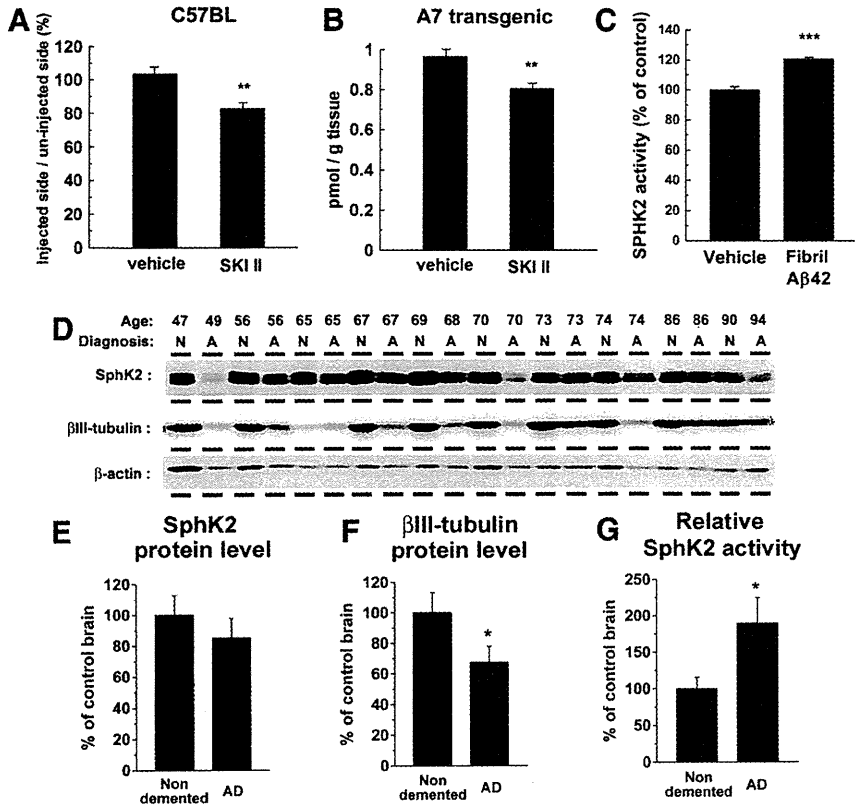

Figure 7. Role of SphK2 activity in AD brains. ***A***, Effect of the direct injection of SKI II into the hippocampus of nontransgenic wild-type female mice (C57BL) at 8 weeks of age. The levels of Tris-soluble Aβ in the injected side of hippocampus were divided by those in the uninjected side. Data represent relative ratio of each group ($n = 4$; mean ± SEM; $^{**}p < 0.01$). ***B***, Levels of Tris-soluble Aβ in the cerebral cortices of female A7 mice at 6 months of age after a 7 d treatment with SKI II (50 mg · kg^{-1} · d^{-1}, p.o.). Total brain Aβ levels were measured by human-specific sandwich ELISA ($n = 5$; mean ± SEM; $^{**}p < 0.01$). ***C***, Effect of Aβ fibril on SphK2 activity in N2a cells. N2a cells were treated with $A\beta_{42}$ fibril (30 μM) overnight, and cell lysates were subjected to an *in vitro* SphK2 activity assay ($n = 3$; mean ± SEM; $^{***}p < 0.001$). ***D–F***, Immunoblot analysis of Tris-soluble fractions (15 μg of protein in each lane) from cortices of AD (denoted as A) or non-demented (denoted as N) individuals. Average protein levels of SphK2 (***E***) and βIII-tubulin (***F***) in each individual were analyzed by densitometric analyses ($^{*}p < 0.05$). ***G***, Average of *in vitro* SphK2 enzymatic activity of Tris-soluble fractions from brains of AD and non-demented individuals. The enzymatic activities of SphK2 were normalized by the protein levels of SphK2 quantified in ***D***.

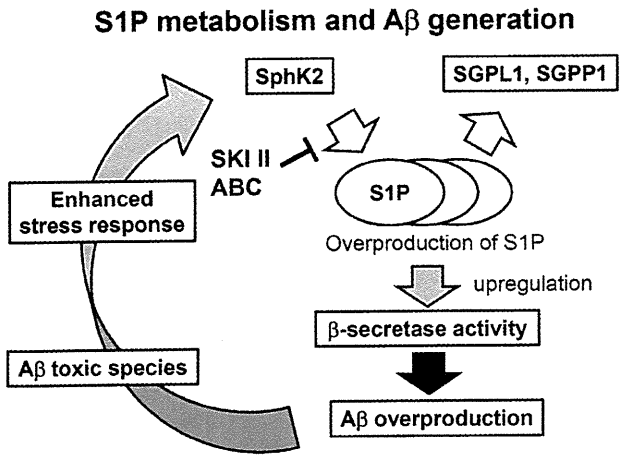

Figure 8. Schematic representation of the role of S1P metabolism in AD.

transgenic mouse brains has beneficial effects against Aβ production.

SphK activity is regulated by various stimuli and stress (Spiegel and Milstien, 2007). Intriguingly, treatment of N2a cells with fibrillized $A\beta_{42}$ caused a significant increase in the SphK2 activity (Fig. 7*C*), raising the possibility that the Aβ deposits in AD brains in turn augment Aβ production through SphK-mediated BACE1 activation in neurons. To further clarify the significance of SphK2 activity in the pathogenesis of sporadic AD, we compared the protein levels and the activities of SphK2 in cerebral cortices between sporadic AD patients and non-demented individuals (Fig. 7*D*). In contrast to the levels of α-actin, the levels of neuronal βIII-tubulin were significantly decreased in AD brains because of neuronal loss (Hempen and Brion, 1996). The protein levels of SphK2 also showed a decreased trend in AD brains (Fig. 7*E,F*), in accord with the previous description that the major SphK2-expressing cells are neurons (Blondeau et al., 2007). However, the relative *in vitro* activities of SphK2 were significantly upregulated in AD brains (Fig. 7*G*). These results provide compelling evidence that changes in the levels of cell-associated S1P in neurons, which is increased by a variety of stimuli including Aβ fibrils, modulate the proteolytic activity of BACE1, thereby forming a vicious cycle in the etiology of AD (Fig. 8).

Discussion

Here we show that lowering the activity of SphK or increasing that of S1P degrading enzymes decreased the Aβ production by the inhibition of BACE1 activity *in vitro* and *in vivo*. Notably, SphK2 activity was increased by exposing cells to Aβ fibrils, and it also was increased in the postmortem cerebral cortices of AD patients. These results suggest that SphK2 and S1P are involved in the etiology of AD and novel potential therapeutic targets for AD.

Metabolites of sphingolipids are functionally interrelated with each other. Inhibition of SphK activity diminishes the generation of S1P and simultaneously increases the cellular levels of sphingosine and ceramide (Spiegel and Milstien, 2007; Pyne and Pyne, 2010). However, overexpression of SGPP1 or SGPL1, which decreases S1P levels by dephosphorylation or irreversible degradation, also decreased the levels of Aβ in N2a cells (Fig. 5). Moreover, direct addition of S1P to the membrane, but not on living cells, increased the β-secretase activity, suggesting that the cell-associated form of S1P per se plays a critical role for the modulation of BACE1 activity in neurons. Importantly, we observed a specific interaction of S1P with BACE1 holoprotein (Fig. 6*F*), in which transmembrane and intracellular domains of BACE1 are required (Fig. 6*G*). Thus, we hypothesize that S1P binds to BACE1 transmembrane/intracellular domain (Fig. 6*H*) and affects the proteolytic activity by altering the conformation or substrate accessibility. In good accordance with this, recent findings implicate intracellular S1P as a novel modulator for enzymes; S1P specifically binds to the histone deacetylases HDAC1 and HDAC2 and inhibited their enzymatic activity (Hait et al., 2009). Moreover, S1P targets to TRAF2 at the RING domain to

stimulate E3 ligase activity (Alvarez et al., 2010). It has been shown that functions of membrane-embedded as well as membrane-associated proteins are modulated by direct interaction with sphingolipids [e.g., activation of TrkA receptor by GM1 (Mutoh et al., 1995), inhibition of epidermal growth factor receptor by GM3 (Kawashima et al., 2009), activation of synaptobrevin (Darios et al., 2009), and functional modulation of stargazin by sphingosine (Sumioka et al., 2010)]. In these cases, lipid interactions are predicted to affect the conformation of functionally active domains located at the luminal or cytoplasmic sides. Moreover, it was shown previously that RTN3 inhibits the BACE1 activity via interaction with the transmembrane domain of BACE1 (He et al., 2004; Murayama et al., 2006). In addition, we have recently identified that a lipophilic, noncompetitive BACE1 inhibitor, TAK-070, directly targets the transmembrane domain of BACE1 (Fukumoto et al., 2010). These results collectively support the notion that targeting the transmembrane domain of BACE1, which harbors an allosteric modulatory function on the catalytic domain, might be a novel approach for the inhibition of the β-cleavage. Additional detailed analysis of molecular effects of S1P on BACE1 should be performed.

Several reports indicate that intrinsic activity of BACE1 is increased in AD brains (Fukumoto et al., 2002; Yang et al., 2003; Li et al., 2004; Ahmed et al., 2010), although the underlying molecular mechanism is essentially unknown. In this study, we found that treatment of cultured cells with Aβ fibrils augmented SphK2 activity, which was increased in AD brains, as well. Notably, intrinsic SphK2 activity is modulated by extracellular signal-regulated kinase (ERK) and fyn kinase (Olivera et al., 2006; Hait et al., 2007), which have been implicated in Aβ-mediated neurotoxicity (Crews and Masliah, 2010), suggesting the possibility that upregulation of SphK2 activity was mediated by aberrant phosphorylation by ERK and/or fyn kinase activity. Additional analysis would be required to understand the molecular connection between Aβ and SphK2 activity. Moreover, SphK2 activity was upregulated by neuronal stress, such as ischemia (Blondeau et al., 2007), which is also correlated with modulation of BACE1 activity (Wen et al., 2004; Tesco et al., 2007). Nevertheless, the increased SphK2 activity by Aβ fibril in neurons thereby may form a vicious cycle in the pathophysiology of AD (Fig. 8). Finally, SKI II treatment decreased the brain Aβ levels in APP transgenic mice, supporting the feasibility of SphK inhibition as a potential AD therapy. Especially, SphK2 single knock-out mice did not show significant developmental defects (Mizugishi et al., 2005). Moreover, SphK2 has been implicated in proapoptotic function, whereas SphK1 harbors anti-apoptotic effects (Liu et al., 2003; Maceyka et al., 2005). Thus, SphK2 selective inhibitors, e.g., ABC294640 (French et al., 2010), may be tolerable and suitable therapeutic agents for AD therapeutics. In conclusion, SphK2/S1P in brain might be a novel molecular target for AD therapeutics, and additional analysis for the regulatory mechanisms of β-secretase activity by SphK/S1P will facilitate the understanding of the pathogenesis of sporadic AD.

References

Ahmed RR, Holler CJ, Webb RL, Li F, Beckett TL, Murphy MP (2010) BACE1 and BACE2 enzymatic activities in Alzheimer's disease. J Neurochem 112:1045–1053.

Alvarez SE, Milstien S, Spiegel S (2007) Autocrine and paracrine roles of sphingosine-1-phosphate. Trends Endocrinol Metab 18:300–307.

Alvarez SE, Harikumar KB, Hait NC, Allegood J, Strub GM, Kim EY, Maceyka M, Jiang H, Luo C, Kordula T, Milstien S, Spiegel S (2010) Sphingosine-1-phosphate is a missing cofactor for the E3 ubiquitin ligase TRAF2. Nature 465:1084–1088.

Arnold SE, Lee EB, Moberg PJ, Stutzbach L, Kazi H, Han LY, Lee VM, Trojanowski JQ (2010) Olfactory epithelium amyloid-β and paired helical filament-tau pathology in Alzheimer disease. Ann Neurol 67:462–469.

Blondeau N, Lai Y, Tyndall S, Popolo M, Topalkara K, Pru JK, Zhang L, Kim H, Liao JK, Ding K, Waeber C (2007) Distribution of sphingosine kinase activity and mRNA in rodent brain. J Neurochem 103:509–517.

Cai H, Wang Y, McCarthy D, Wen H, Borchelt DR, Price DL, Wong PC (2001) BACE1 is the major beta-secretase for generation of Aβ peptides by neurons. Nat Neurosci 4:233–234.

Chow VW, Savonenko AV, Melnikova T, Kim H, Price DL, Li T, Wong PC (2010) Modeling an anti-amyloid combination therapy for Alzheimer's disease. Sci Transl Med 2:13ra1.

Crews L, Masliah E (2010) Molecular mechanisms of neurodegeneration in Alzheimer's disease. Hum Mol Genet 19:R12–R20.

Darios F, Wasser C, Shakirzyanova A, Giniatullin A, Goodman K, Munoz-Bravo JL, Raingo J, Jorgacevski J, Kreft M, Zorec R, Rosa JM, Gandia L, Gutiérrez LM, Binz T, Giniatullin R, Kavalali ET, Davletov B (2009) Sphingosine facilitates SNARE complex assembly and activates synaptic vesicle exocytosis. Neuron 62:683–694.

De Strooper B, Vassar R, Golde T (2010) The secretases: enzymes with therapeutic potential in Alzheimer disease. Nat Rev Neurol 6:99–107.

Don AS, Martinez-Lamenca C, Webb WR, Proia RL, Roberts E, Rosen H (2007) Essential requirement for sphingosine kinase 2 in a sphingolipid apoptosis pathway activated by FTY720 analogues. J Biol Chem 282:15833–15842.

French KJ, Schrecengost RS, Lee BD, Zhuang Y, Smith SN, Eberly JL, Yun JK, Smith CD (2003) Discovery and evaluation of inhibitors of human sphingosine kinase. Cancer Res 63:5962–5969.

French KJ, Upson JJ, Keller SN, Zhuang Y, Yun JK, Smith CD (2006) Antitumor activity of sphingosine kinase inhibitors. J Pharmacol Exp Ther 318:596–603.

French KJ, Zhuang Y, Maines LW, Gao P, Wang W, Beljanski V, Upson JJ, Green CL, Keller SN, Smith CD (2010) Pharmacology and antitumor activity of ABC294640, a selective inhibitor of sphingosine kinase-2. J Pharmacol Exp Ther 333:129–139.

Fukumoto H, Tomita T, Matsunaga H, Ishibashi Y, Saido TC, Iwatsubo T (1999) Primary cultures of neuronal and non-neuronal rat brain cells secrete similar proportions of amyloid β peptides ending at Aβ40 and Aβ42. Neuroreport 10:2965–2969.

Fukumoto H, Cheung BS, Hyman BT, Irizarry MC (2002) β-secretase protein and activity are increased in the neocortex in Alzheimer disease. Arch Neurol 59:1381–1389.

Fukumoto H, Takahashi H, Tarui N, Matsui J, Tomita T, Hirode M, Sagayama M, Maeda R, Kawamoto M, Hirai K, Terauchi J, Sakura Y, Kakihana M, Kato K, Iwatsubo T, Miyamoto M (2010) A noncompetitive BACE1 inhibitor TAK-070 ameliorates Aβ pathology and behavioral deficits in a mouse model of Alzheimer's disease. J Neurosci 30:11157–11166.

Hait NC, Bellamy A, Milstien S, Kordula T, Spiegel S (2007) Sphingosine kinase type 2 activation by ERK-mediated phosphorylation. J Biol Chem 282:12058–12065.

Hait NC, Allegood J, Maceyka M, Strub GM, Harikumar KB, Singh SK, Luo C, Marmorstein R, Kordula T, Milstien S, Spiegel S (2009) Regulation of histone acetylation in the nucleus by sphingosine-1-phosphate. Science 325:1254–1257.

Hashimoto T, Wakabayashi T, Watanabe A, Kowa H, Hosoda R, Nakamura A, Kanazawa I, Arai T, Takio K, Mann DM, Iwatsubo T (2002) CLAC: a novel Alzheimer amyloid plaque component derived from a transmembrane precursor, CLAC-P/collagen type XXV. EMBO J 21:1524–1534.

He W, Lu Y, Qahwash I, Hu XY, Chang A, Yan R (2004) Reticulon family members modulate BACE1 activity and amyloid-β peptide generation. Nat Med 10:959–965.

Hempen B, Brion JP (1996) Reduction of acetylated α-tubulin immunoreactivity in neurofibrillary tangle-bearing neurons in Alzheimer's disease. J Neuropathol Exp Neurol 55:964–972.

Hori Y, Hashimoto T, Wakutani Y, Urakami K, Nakashima K, Condron MM, Tsubuki S, Saido TC, Teplow DB, Iwatsubo T (2007) The Tottori (D7N) and English (H6R) familial Alzheimer disease mutations accelerate Aβ fibril formation without increasing protofibril formation. J Biol Chem 282:4916–4923.

Hu X, Hicks CW, He W, Wong P, Macklin WB, Trapp BD, Yan R (2006) Bace1 modulates myelination in the central and peripheral nervous system. Nat Neurosci 9:1520–1525.

Hu X, Zhou X, He W, Yang J, Xiong W, Wong P, Wilson CG, Yan R (2010) BACE1 deficiency causes altered neuronal activity and neurodegeneration. J Neurosci 30:8819–8829.

Iwatsubo T, Odaka A, Suzuki N, Mizusawa H, Nukina N, Ihara Y (1994) Visualization of Aβ42(43) and Aβ40 in senile plaques with end-specific Aβ monoclonals: evidence that an initially deposited species is Aβ42(43). Neuron 13:45–53.

Kalvodova L, Kahya N, Schwille P, Ehehalt R, Verkade P, Drechsel D, Simons K (2005) Lipids as modulators of proteolytic activity of BACE: involvement of cholesterol, glycosphingolipids, and anionic phospholipids *in vitro*. J Biol Chem 280:36815–36823.

Kan T, Tominari Y, Morohashi Y, Natsugari H, Tomita T, Iwatsubo T, Fukuyama T (2003) Solid-phase synthesis of photoaffinity probes: highly efficient incorporation of biotin-tag and cross-linking groups. Chem Commun (Camb) 2244–2245.

Kawashima N, Yoon SJ, Itoh K, Nakayama K (2009) Tyrosine kinase activity of epidermal growth factor receptor is regulated by GM3 binding through carbohydrate to carbohydrate interactions. J Biol Chem 284:6147–6155.

Kihara A, Ikeda M, Kariya Y, Lee EY, Lee YM, Igarashi Y (2003) Sphingosine-1-phosphate lyase is involved in the differentiation of F9 embryonal carcinoma cells to primitive endoderm. J Biol Chem 278:14578–14585.

Kopan R, Schroeter EH, Weintraub H, Nye JS (1996) Signal transduction by activated mNotch: importance of proteolytic processing and its regulation by the extracellular domain. Proc Natl Acad Sci U S A 93:1683–1688.

Laird FM, Cai H, Savonenko AV, Farah MH, He K, Melnikova T, Wen H, Chiang HC, Xu G, Koliatsos VE, Borchelt DR, Price DL, Lee HK, Wong PC (2005) BACE1, a major determinant of selective vulnerability of the brain to amyloid-β amyloidogenesis, is essential for cognitive, emotional, and synaptic functions. J Neurosci 25:11693–11709.

Li R, Lindholm K, Yang LB, Yue X, Citron M, Yan R, Beach T, Sue L, Sabbagh M, Cai H, Wong P, Price D, Shen Y (2004) Amyloid β peptide load is correlated with increased β-secretase activity in sporadic Alzheimer's disease patients. Proc Natl Acad Sci U S A 101:3632–3637.

Liu H, Toman RE, Goparaju SK, Maceyka M, Nava VE, Sankala H, Payne SG, Bektas M, Ishii I, Chun J, Milstien S, Spiegel S (2003) Sphingosine kinase type 2 is a putative BH3-only protein that induces apoptosis. J Biol Chem 278:40330–40336.

Luo Y, Bolon B, Kahn S, Bennett BD, Babu-Khan S, Denis P, Fan W, Kha H, Zhang J, Gong Y, Martin L, Louis JC, Yan Q, Richards WG, Citron M, Vassar R (2001) Mice deficient in BACE1, the Alzheimer's β-secretase, have normal phenotype and abolished β-amyloid generation. Nat Neurosci 4:231–232.

Maceyka M, Sankala H, Hait NC, Le Stunff H, Liu H, Toman R, Collier C, Zhang M, Satin LS, Merrill AH Jr, Milstien S, Spiegel S (2005) SphK1 and SphK2, sphingosine kinase isoenzymes with opposing functions in sphingolipid metabolism. J Biol Chem 280:37118–37129.

McConlogue L, Buttini M, Anderson JP, Brigham EF, Chen KS, Freedman SB, Games D, Johnson-Wood K, Lee M, Zeller M, Liu W, Motter R, Sinha S (2007) Partial reduction of BACE1 has dramatic effects on Alzheimer plaque and synaptic pathology in APP transgenic mice. J Biol Chem 282:26326–26334.

Mizugishi K, Yamashita T, Olivera A, Miller GF, Spiegel S, Proia RL (2005) Essential role for sphingosine kinases in neural and vascular development. Mol Cell Biol 25:11113–11121.

Murayama KS, Kametani F, Saito S, Kume H, Akiyama H, Araki W (2006) Reticulons RTN3 and RTN4-B/C interact with BACE1 and inhibit its ability to produce amyloid β-protein. Eur J Neurosci 24:1237–1244.

Mutoh T, Tokuda A, Miyadai T, Hamaguchi M, Fujiki N (1995) Ganglioside GM1 binds to the Trk protein and regulates receptor function. Proc Natl Acad Sci U S A 92:5087–5091.

Olivera A, Urtz N, Mizugishi K, Yamashita Y, Gilfillan AM, Furumoto Y, Gu H, Proia RL, Baumruker T, Rivera J (2006) IgE-dependent activation of sphingosine kinases 1 and 2 and secretion of sphingosine 1-phosphate requires Fyn kinase and contributes to mast cell responses. J Biol Chem 281:2515–2525.

Pyne NJ, Pyne S (2010) Sphingosine 1-phosphate and cancer. Nat Rev Cancer 10:489–503.

Rajendran L, Schneider A, Schlechtingen G, Weidlich S, Ries J, Braxmeier T, Schwille P, Schulz JB, Schroeder C, Simons M, Jennings G, Knölker HJ, Simons K (2008) Efficient inhibition of the Alzheimer's disease β-secretase by membrane targeting. Science 320:520–523.

Reiss U, Oskouian B, Zhou J, Gupta V, Sooriyakumaran P, Kelly S, Wang E, Merrill AH Jr, Saba JD (2004) Sphingosine-phosphate lyase enhances stress-induced ceramide generation and apoptosis. J Biol Chem 279:1281–1290.

Savonenko AV, Melnikova T, Laird FM, Stewart KA, Price DL, Wong PC (2008) Alteration of BACE1-dependent NRG1/ErbB4 signaling and schizophrenia-like phenotypes in BACE1-null mice. Proc Natl Acad Sci U S A 105:5585–5590.

Schwab SR, Pereira JP, Matloubian M, Xu Y, Huang Y, Cyster JG (2005) Lymphocyte sequestration through S1P lyase inhibition and disruption of S1P gradients. Science 309:1735–1739.

Spiegel S, Milstien S (2007) Functions of the multifaceted family of sphingosine kinases and some close relatives. J Biol Chem 282:2125–2129.

Sumioka A, Yan D, Tomita S (2010) TARP phosphorylation regulates synaptic AMPA receptors through lipid bilayers. Neuron 66:755–767.

Takabe K, Paugh SW, Milstien S, Spiegel S (2008) "Inside-out" signaling of sphingosine-1-phosphate: therapeutic targets. Pharmacol Rev 60:181–195.

Takasugi N, Tomita T, Hayashi I, Tsuruoka M, Niimura M, Takahashi Y, Thinakaran G, Iwatsubo T (2003) The role of presenilin cofactors in the γ-secretase complex. Nature 422:438–441.

Tesco G, Koh YH, Kang EL, Cameron AN, Das S, Sena-Esteves M, Hiltunen M, Yang SH, Zhong Z, Shen Y, Simpkins JW, Tanzi RE (2007) Depletion of GGA3 stabilizes BACE and enhances β-secretase activity. Neuron 54:721–737.

Tomita T (2009) Secretase inhibitors and modulators for Alzheimer's disease treatment. Expert Rev Neurother 9:661–679.

Tomita T, Maruyama K, Saido TC, Kume H, Shinozaki K, Tokuhiro S, Capell A, Walter J, Grünberg J, Haass C, Iwatsubo T, Obata K (1997) The presenilin 2 mutation (N141I) linked to familial Alzheimer disease (Volga German families) increases the secretion of amyloid β protein ending at the 42nd (or 43rd) residue. Proc Natl Acad Sci U S A 94:2025–2030.

Tomita T, Takikawa R, Koyama A, Morohashi Y, Takasugi N, Saido TC, Maruyama K, Iwatsubo T (1999) C terminus of presenilin is required for overproduction of amyloidogenic Aβ42 through stabilization and endoproteolysis of presenilin. J Neurosci 19:10627–10634.

Vassar R, Kovacs DM, Yan R, Wong PC (2009) The beta-secretase enzyme BACE in health and Alzheimer's disease: regulation, cell biology, function, and therapeutic potential. J Neurosci 29:12787–12794.

Vetrivel KS, Thinakaran G (2010) Membrane rafts in Alzheimer's disease β-amyloid production. Biochim Biophys Acta 1801:860–867.

Wen Y, Onyewuchi O, Yang S, Liu R, Simpkins JW (2004) Increased β-secretase activity and expression in rats following transient cerebral ischemia. Brain Res 1009:1–8.

Willem M, Garratt AN, Novak B, Citron M, Kaufmann S, Rittger A, DeStrooper B, Saftig P, Birchmeier C, Haass C (2006) Control of peripheral nerve myelination by the β-secretase BACE1. Science 314:664–666.

Yamada K, Yabuki C, Seubert P, Schenk D, Hori Y, Ohtsuki S, Terasaki T, Hashimoto T, Iwatsubo T (2009) Aβ immunotherapy: intracerebral sequestration of Aβ by an anti-Aβ monoclonal antibody 266 with high affinity to soluble Aβ. J Neurosci 29:11393–11398.

Yang LB, Lindholm K, Yan R, Citron M, Xia W, Yang XL, Beach T, Sue L, Wong P, Price D, Li R, Shen Y (2003) Elevated β-secretase expression and enzymatic activity detected in sporadic Alzheimer disease. Nat Med 9:3–4.

Yoshimoto T, Furuhata M, Kamiya S, Hisada M, Miyaji H, Magami Y, Yamamoto K, Fujiwara H, Mizuguchi J (2003) Positive modulation of IL-12 signaling by sphingosine kinase 2 associating with the IL-12 receptor beta 1 cytoplasmic region. J Immunol 171:1352–1359.

Zemann B, Kinzel B, Müller M, Reuschel R, Mechtcheriakova D, Urtz N, Bornancin F, Baumruker T, Billich A (2006) Sphingosine kinase type 2 is essential for lymphopenia induced by the immunomodulatory drug FTY720. Blood 107:1454–1458.

Oncogene (2011) 1–12
© 2011 Macmillan Publishers Limited All rights reserved 0950-9232/11
www.nature.com/onc

ORIGINAL ARTICLE

Neutralization of the γ-secretase activity by monoclonal antibody against extracellular domain of nicastrin

I Hayashi[1,10], S Takatori[1,10], Y Urano[2,9], Y Miyake[3], J Takagi[4], M Sakata-Yanagimoto[3], H Iwanari[2,5], S Osawa[1], Y Morohashi[1], T Li[6], PC Wong[6], S Chiba[3], T Kodama[2], T Hamakubo[2], T Tomita[1,7] and T Iwatsubo[1,7,8]

[1]Department of Neuropathology and Neuroscience, Graduate School of Pharmaceutical Sciences, The University of Tokyo, Tokyo, Japan; [2]Department of Systems Biology and Medicine, Research Center for Advanced Science and Technology, The University of Tokyo, Tokyo, Japan; [3]Department of Clinical and Experimental Hematology, Graduate School of Comprehensive Human Sciences, University of Tsukuba, Tsukuba, Japan; [4]Laboratory of Protein Synthesis and Expression, Institute for Protein Research, Osaka University, Osaka, Japan; [5]Perseus Proteomics Inc., Tokyo, Japan; [6]Department of Pathology, The Johns Hopkins University, School of Medicine, Baltimore, MD, USA; [7]Core Research for Evolutional Science and Technology, Japan Science and Technology Agency, Saitama, Japan and [8]Department of Neuropathology, Graduate School of Medicine, The University of Tokyo, Tokyo, Japan

Several lines of evidence suggest that aberrant Notch signaling contributes to the development of several types of cancer. Activation of Notch receptor is executed through intramembrane proteolysis by γ-secretase, which is a multimeric membrane-embedded protease comprised of presenilin, nicastrin (NCT), anterior pharynx defective 1 and PEN-2. In this study, we report the neutralization of the γ-secretase activity by a novel monoclonal antibody A5226A against the extracellular domain of NCT, generated by using a recombinant budded baculovirus as an immunogen. This antibody recognized fully glycosylated mature NCT in the active γ-secretase complex on the cell surface, and inhibited the γ-secretase activity by competing with the substrate binding *in vitro*. Moreover, A5226A abolished the γ-secretase activity-dependent growth of cancer cells in a xenograft model. Our data provide compelling evidence that NCT is a molecular target for the mechanism-based inhibition of γ-secretase, and that targeting NCT might be a novel therapeutic strategy against cancer caused by aberrant γ-secretase activity and Notch signaling.

Oncogene advance online publication, 4 July 2011; doi:10.1038/onc.2011.265

Keywords: Notch; γ-secretase; functional antibody; membrane protein; intramembrane cleavage

Introduction

Notch is a membrane-bound transcription factor that regulates metazoan developmental program (Kopan and Ilagan, 2009). After the interaction with its ligand, Notch is endoproteolyzed by an intramembrane cleaving enzyme, γ-secretase, to liberate the Notch intracellular domain that translocates into the nucleus and activates the transcription of downstream target genes. Recent studies suggest that alterations of Notch signaling contribute to cancer development. Notably, activating mutations of *NOTCH1* account for over 50% of human T-cell acute lymphoblastic leukemia (Ferrando, 2009). These mutations result in ligand-independent generation or prolonged existence of Notch intracellular domain, which causes upregulation of Notch signaling. Also, aberrant Notch signaling has been implicated in tumorigenesis of glioma, colon, pancreatic, non-small cell lung and breast cancers (Pannuti *et al.*, 2010; Yin *et al.*, 2010). It has been reported that treatment with γ-secretase inhibitors causes a dramatic decrease in the proliferation of these cancer models (van Es and Clevers, 2005; Fan *et al.*, 2006; Kimura *et al.*, 2007; Osipo *et al.*, 2008; Luistro *et al.*, 2009). Moreover, Notch signaling contributes to angiogenesis in solid tumors as well as drug resistance against chemotherapy. Thus, modulation of Notch signaling could be used in the treatment of these cancers.

Monoclonal antibody (mAb)-based anti-cancer strategy has been developed and now is widely used in clinics (Samaranayake *et al.*, 2009; Weiner *et al.*, 2010). Especially, mAbs exhibit several advantages compared with small compounds; long half-life and multiple immunological mechanisms, including antibody-dependent cell-mediated cytotoxicity, have been implicated in the anti-cancer effects of therapeutic mAbs. Moreover, functional mAbs with antagonistic effects on the target molecule also have been developed as therapeutic mAbs (for example, trastuzumab for HER2, cetuximab for EGFR, tocilizumab for IL-6R). Intriguingly, some of the target molecules are enzymes working within the cell

Correspondence: Dr T Tomita, Department of Neuropathology and Neuroscience, Graduate School of Pharmaceutical Sciences, The University of Tokyo, 7-3-1 Hongo, Bunkyo-ku, Tokyo 113-0033, Japan.
E-mail: taisuke@mol.f.u-tokyo.ac.jp
[9]Present address: Department of Medical Life Systems, Graduate School of Life and Medical Sciences, Doshisha University, 1-3 Tatara Miyakodani, Kyotanabe, Kyoto 610-0394, Japan.
[10]These authors equally contributed to this study.
Received 10 October 2010; revised 31 May 2011; accepted 31 May 2011

(that is, receptor tyrosine kinase). In such cases, a combination strategy using a therapeutic mAb and a small compound inhibitor against the same target is expected to be therapeutically effective (Samaranayake *et al.*, 2009). However, several difficulties underlie the development of mAbs that react with proteins in a functional state. In general, proper folding and post-translational modifications in extracellular domain (ECD) of the membrane protein are required for its function, while a significant proportion of overexpressed recombinant proteins tends to misfold and aggregate without forming proper tertiary structures. We have developed a novel membrane protein expression and immunization system using budded baculoviral particles, which are able to display biologically active membrane proteins including the γ-secretase complex on viral virions (Masuda *et al.*, 2003; Urano *et al.*, 2003; Hayashi *et al.*, 2004; Saitoh *et al.*, 2006). Using this technology, we have successfully obtained several mAbs that recognize peptide transporters and G-protein-coupled receptors in a functional conformation (Saitoh *et al.*, 2007).

γ-Secretase is responsible for the intramembrane proteolysis of various type I transmembrane proteins including Notch as well as amyloid precursor protein, the latter being a precursor for amyloid-β peptide that is implicated in the pathogenesis of Alzheimer disease (Tomita, 2009; De Strooper *et al.*, 2010). To date, however, mAbs against the γ-secretase complex that inhibit the proteolytic activity have not been reported, while several potent γ-secretase inhibitors have been identified. γ-Secretase is a multimeric membrane protein complex comprised of presenilin (PS), nicastrin (NCT), anterior pharynx defective 1 (APH-1) and PEN-2. PS is the catalytic subunit that forms the hydrophilic catalytic pore buried within the membrane (Takasugi *et al.*, 2003). Importantly, several γ-secretase inhibitors identified so far directly target PS, while other components are also indispensable for the physiological γ-secretase activity (Tomita, 2009). Among these subunits, NCT is a type I membrane glycoprotein with a large ECD. During the proteolytic process, NCT ECD captures the N terminus of the substrate as a primary substrate receptor (that is exosite) for γ-secretase (Shah *et al.*, 2005). In the present study, we identified a mAb A5226A that recognizes NCT ECD as a neutralizing mAb against the intramembrane proteolysis by the γ-secretase. We also showed a therapeutic potential of A5226A against proliferation of cancer cells, in which aberrant activation of the γ-secretase activity-dependent signaling is involved.

Results

Biochemical characterization of anti-NCT mAbs A5201A and A5226A

To generate functional mAbs that modulate the γ-secretase activities, we chose NCT as a target protein among the four known components for the following reasons: (i) NCT has a large ECD that is expected to be displayed on the surface of budded baculovirus, (ii) NCT has been reported to function as a substrate receptor (Shah *et al.*, 2005). We immunized gp64 transgenic mice with NCT-expressing budded baculovirus and obtained a dozen of positive hybridoma clones. We further characterized two anti-NCT mAbs (A5201A and A5226A), which showed a high titer against NCT ECD (Figure 1a). NCT undergoes maturation process including endoglycosidase H-resistant, complex-type *N*-glycosylation and acquiring a trypsin resistance during the assembly of the γ-secretase complex (Yu *et al.*, 2000; Esler *et al.*, 2002; Tomita *et al.*, 2002; Shirotani *et al.*, 2003; Hayashi *et al.*, 2009). Only the mature form of NCT is detected in the functionally active γ-secretase complex at late secretory pathway including cell surface (Kaether *et al.*, 2002), while the immature form of NCT forms a subcomplex with APH-1 at endoplasmic reticulum (LaVoie *et al.*, 2003). On immunoblot analysis, both mAbs specifically reacted with both mature and immature forms of human NCT overexpressed in fibroblasts from *Ncstn* knockout mouse (NKO cells) (Figure 1b). Intriguingly, both mAbs reacted exclusively with human NCT but not with that of other species (that is mouse, rat, chicken and fruit fly) (Supplementary Figure 1A–C). These mAbs recognized endoglycosidase H- as well as PNGase-treated deglycosylated NCT, the latter lacking all *N*-glycosylation, although the reactivity against deglycosylated NCT was considerably reduced (Figures 1c and d). Collectively, these data suggest that the major epitopes for these mAbs are located on NCT polypeptide, and that the sugar chains attached to NCT might be involved in the recognition by the mAbs.

To investigate the reactivities of these mAbs against NCT under a condition where the integrity of the γ-secretase complex is preserved, immunoprecipitation experiments were performed. Surprisingly, A5201A precipitated only the immature form of NCT, whereas A5226A bound to both mature and immature NCT (Figures 2a and b). In accordance with this observation, A5226A precipitated all the other components of the γ-secretase complex, that is, PS1, APH-1aL and PEN-2. In contrast, A5201A precipitated only APH-1aL, indicating that A5201A specifically binds immature NCT as well as NCT–APH-1 subcomplex (LaVoie *et al.*, 2003). Using a set of deletion mutants (Shirotani *et al.*, 2003) (Figure 2c), we found that epitopes for these mAbs reside within NCT ECD in a different manner: A5201A showed no binding to any mutants except for NCT/Δ1. In contrast, A5226A failed to react with NCT/Δ4 lacking amino acid residues 361–516 of NCT, while the reactivity against the other deletion mutants was significantly reduced (Figure 2d). Considering previous reports that NCT ECD undergoes a conformational change during the formation of the active γ-secretase complex, these data suggest that A5201A recognizes a broad region or structure in NCT ECD that is hindered in the mature NCT-containing complex by the conformational change; in contrast, the recognition by A5226A requires a presence of the amino acid residues 361–516, which is accessible in the folded/mature NCT ECD. To further narrow down the epitope of A5226A, we analyzed the reactivity of human and mouse NCT

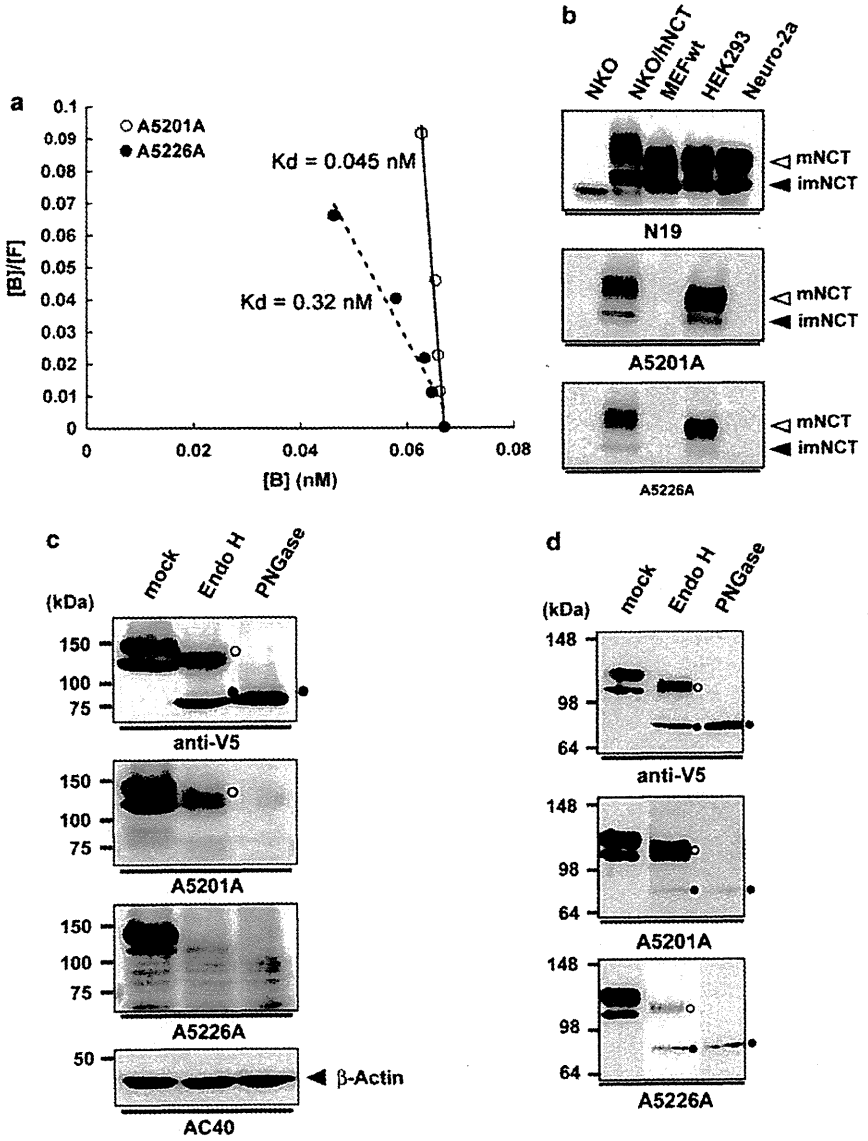

Figure 1 Characterization of anti-NCT mAbs. (**a**) Scatchard plot of A5201A and A5226A. From this plot, Kd value of A5201A and A5226A was calculated as 0.045 and 0.32 nM, respectively. (**b**) Immunoblot analysis of cell lysates using anti-NCT mAbs. Mature and immature forms of NCT are indicated by white and black arrowheads, respectively. Note that only human NCT polypeptides were recognized by A5201A and A5226A. (**c, d**) Reactivity of mAbs against deglycosylated NCT. Immunoreactivities of both A5201A and A5226A were significantly reduced against endoglycosidase H-resistant and -sensitive species of NCT, which are indicated by white and black circles, respectively, in NKO cell lysates incubated with endoglycosidases (**c**). However, both antibodies recognized either the deglycosylated NCT species that was immunoisolated using anti-NCT antibody (**d**).

chimeric polypeptides using sandwich enzyme-linked immunosorbent assay. Preliminary experiments using various human/mouse chimeric NCT revealed that reactivity of A5226A critically depended on the region encompassing residues 333–393. As only six residues (that is K349, Q355, V359, E375, V383 and R391) within this region differed between human and mouse NCT (Figure 2e), we mutated each residues and tested their reactivity with A5226A using the same assay. As shown in Figure 2f, human to mouse mutations K349N, Q355R, V359I, E375D and V383M did not affect the binding of A5226A, while mutation of Arg391 to Lys completely abolished the binding. Conversely, mouse NCT gained full reactivity toward A5226A when K391 was mutated to R. These results clearly indicate that R391 lies at the heart of the binding epitope of A5226A.

A5226A recognizes the functional γ-secretase complex in cholera toxin subunit B (CTB)-positive microdomain at the plasma membrane

Target molecules of the therapeutic mAbs should be located at late secretory pathway including plasma

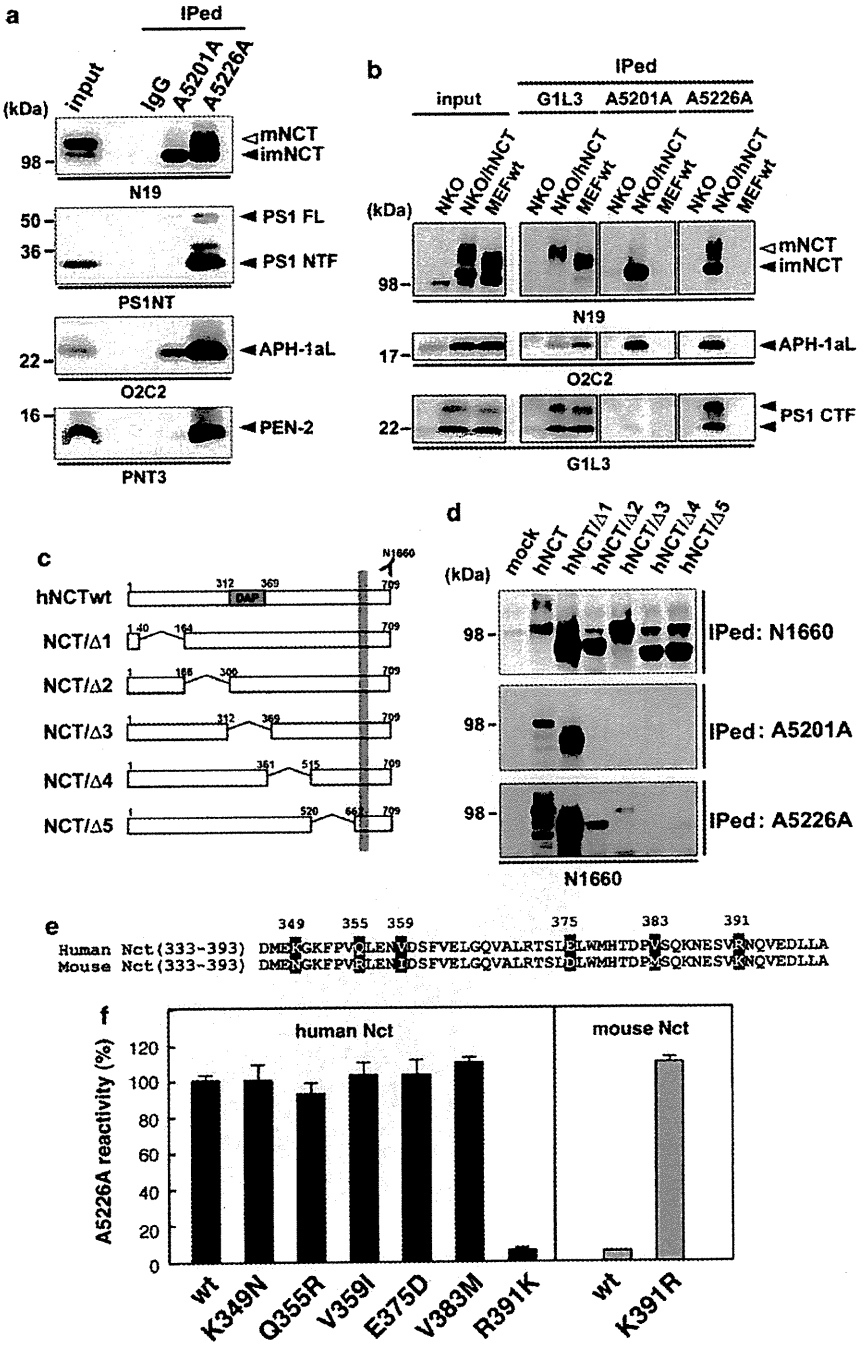

Figure 2 Immunoprecipitation analyses using anti-NCT mAbs. (**a**, **b**) Co-immunoprecipitation of human NCT and the γ-secretase components by anti-NCT mAbs (indicated above the lanes) from CHAPSO-solubilized HeLa (**a**), NKO, NKO expressing human NCT and wild-type MEF (**b**) cell lysates. Immunoblot analyses were performed by antibodies shown below the lanes. Note that A5201A precipitated only immature NCT and APH-1aL, while A5226A captured all components of the γ-secretase complex. (**c**) Schematic depiction of deletion mutants of NCT (Shirotani *et al*., 2003). (**d**) Reactivity of antibodies (shown at the right of the panels) against deletion mutant NCT in immunoprecipitation under the CHAPSO-solubilized condition. All immunoblot analyses were performed by anti-C terminus of NCT antibody N1660. (**e**) Amino-acid sequence of human and mouse NCT around the region containing A5226A epitope. Species-specific residues are shown in black background. (**f**) Reactivity of A5226A toward NCT ectodomain fragments with single-residue substitution. Bindings of biotinylated A5226A toward various hGH-NCT fusion proteins indicated are determined using a sandwich Enzyme-linked immunosorbent assay format, normalized by the expression level deduced from a hGH immunoassay, and expressed as the relative value of the wild-type human NCT. The data shown are the mean of duplicate determinations from a single experiment and are representative of two additional experiments.

membrane. However, precise localization of the active γ-secretase complex still remains unclear, while chemical biology and genetic approaches revealed that Notch cleavage by γ-secretase is occurred at plasma membrane and/or endocytic compartment (Tarassishin *et al.*, 2004; Kopan and Ilagan, 2009). To investigate whether anti-NCT mAbs recognizes endogenous NCT at cell surface, we performed immunocytochemical analysis of non-permeabilized HeLa cells. Intriguingly, immunostaining with A5226A gave a 'scattered patchy' pattern on cell surface unlike that of A5201A, which showed no staining (Figure 3a). We found that this patchy staining was well merged with the staining by CTB, which binds to the pentasaccharide chain of ganglioside GM1 (Boesze-Battaglia, 2006). We further examined subcellular localization of endogenous NCT using permeabilized HeLa cells (Figure 3b). Immunostaining by A5201A resulted in a reticular pattern that merged well with that by an anti-protein disulfide isomerase antibody, suggesting that A5201A specifically recognizes the endoplasmic reticulum-resident, immature NCT under the native condition. However, the CTB-positive patchy dots stained by A5226A were not merged with endoplasmic reticulum or Golgi markers, protein disulfide isomerase or TGN46, respectively, suggesting that A5226A recognizes NCT in CTB-positive microdomain. To confirm that the observed patchy pattern corresponds to the localization of *bona fide* NCT, NKO cells were analyzed (Li *et al.*, 2003) (Figure 3c). Neither of the mAbs showed immunoreactivities in NKO cells. In contrast, in NKO cells expressing human NCT, A5201A and A5226A stained the reticular and patchy structure, respectively, in a similar fashion to those observed in HeLa cells. Moreover, A5226A-positive patch was well merged with the immunoreactivity of anti-PS1 mAb, suggesting that the functional γ-secretase complex resides at GM1-positive membrane microdomain (Figure 3d). In good accordance with these results, several biochemical analyses revealed that the mature form of NCT as well as the γ-secretase activity was fractionated in lipid rafts, where sphingolipids were enriched (Urano *et al.*, 2005; Vetrivel and Thinakaran, 2010). Finally, we examined the localization of a direct γ-secretase substrate, NEXT fragment, proteolytically

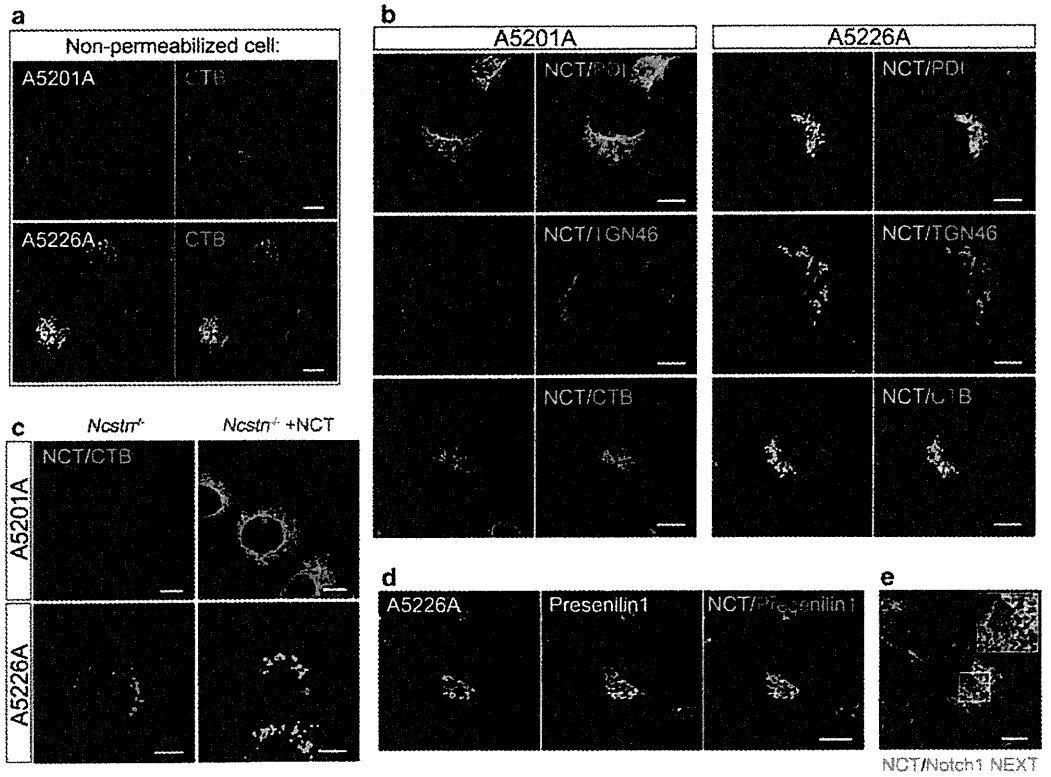

Figure 3 Immunocytochemical analysis using anti-NCT mAbs. (**a**) Immunocytochemical analysis of non-permeabilized HeLa cells using anti-NCT mAbs (green) and CTB (red). These images represent maximum projections of confocal optical sections. (**b**) Immunocytochemical analysis of permeabilized HeLa cells using anti-NCT mAbs (gray scale in left columns and green in merged images) with antibodies against organelle markers (protein disulfide isomerase for ER; TGN46 for TGN) or CTB (red). Note that staining by A5201A and A5226A were well co-localized with that by anti-protein disulfide isomerase and CTB, respectively. (**c**) Specificity of anti-NCT mAbs. Immunocytochemical analysis of NKO (left column) and NKO/hNCT cells (right column) revealed that neither A5201A nor A5226A showed any specific staining in NKO cells. (**d**) Co-immunostaining of permeabilized HeLa cells using A5226A with anti-PS1 antibody. (**e**) Immunocytochemical analysis of DAPT-treated HeLa cells expressing NΔE using A5226A (green) and anti-NOTCH1 NEXT (Val1711) antibody that specifically recognizes S2 cleavage site (red). The higher magnification image of the boxed region is shown in the inset. Nuclei were conter-labeled with DRAQ5 (blue) in all figures. Scale bars: 10 μm.

generated by site 2 cleavage from Notch holoprotein as well as a recombinant Notch-based substrate NΔE. Treatment with γ-secretase inhibitor, *N*-[*N*-(3,5-difluorophenacetyl)-L-alanyl]-(*S*)-phenylglycine *t*-butyl ester (DAPT), caused a significant accumulation of NEXT fragment that was specifically recognized by a Notch1 Val1711 antibody (van Tetering *et al.*, 2009). Intriguingly, NEXT fragments were located in proximity to, and partially co-localized, with the A5226A-positive patch (Figure 3e). Taken together, these data strongly suggest that A5226A specifically recognizes the active γ-secretase complex containing mature NCT localized in CTB-positive microdomain at the plasma membrane.

A5226A neutralizes the γ-secretase activity by inhibition of substrate interaction

Immunocytochemical findings that A5226A labels mature NCT, which constitutes an active γ-secretase complex, at CTB-positive patches on cell surface prompted us to examine whether this mAb affects the γ-secretase activity in living cells. Strikingly, A5226A treatment significantly inhibited the γ-secretase-mediated cleavage in a dose-dependent manner in HEK293 cells stably expressing amyloid precursor protein- or Notch-derived γ-substrate fused with GAL4/UAS system (Imamura *et al.*, 2009) (Figure 4a). Intriguingly, the levels of PS1 fragments were slightly decreased in A5226A-treated cells (Figure 4b). However, the endocytosis rate of mature NCT, PS1 and amyloid precursor protein at cell surface was unchanged by A5226A treatment (Figure 4c). Moreover, the localization of the substrate as well as NCT was not significantly altered by A5226A treatment (data not shown). Nevertheless, further investigation for the molecular mechanism whereby PS1 fragment was decreased by A5226A incubation would be required. Next, we analyzed the effect of A5226A in *in vitro* γ-secretase assay using recombinant substrate. Notably, A5226A decreased intrinsic γ-secretase activity in an *in vitro* assay (Figure 5a). These data indicate that A5226A functions as a neutralizing mAb against the γ-secretase activity. Decreased inhibitory effect of A5226A in *in vitro* assay might be due to difference in requirement of NCT function in proteolytic mechanism of solubilized

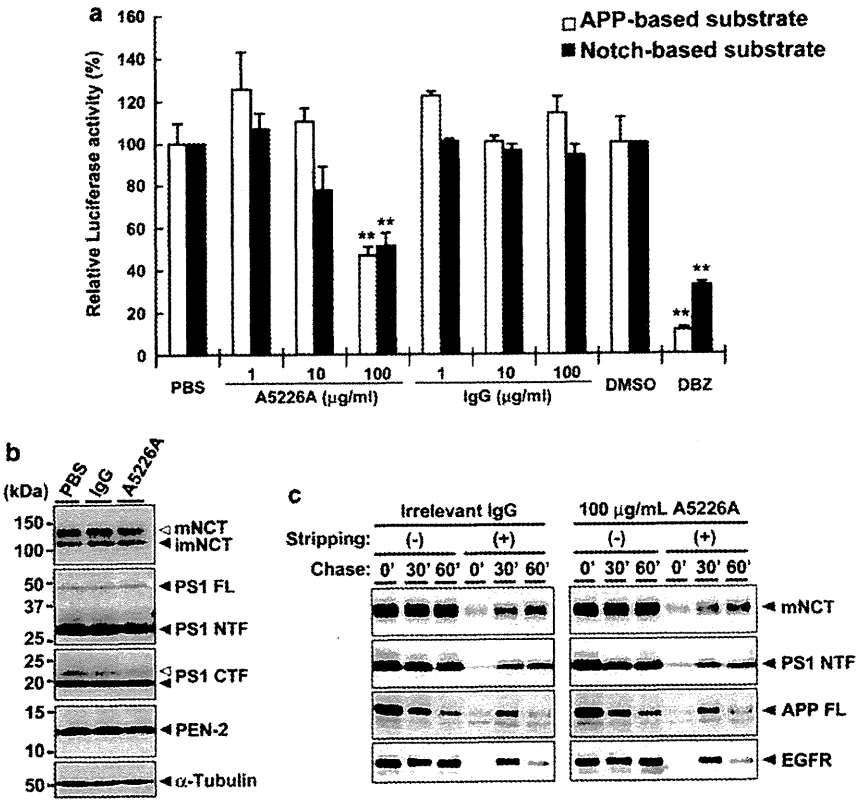

Figure 4 Effect of A5226A treatment on living cells. (**a**) Effects of anti-NCT mAbs in the cell-based γ-secretase assay. Firefly luciferase activity was measured in HEK293 cells stably expressing amyloid precursor protein- (open column) or Notch-based substrate (filled column) fused with GAL4. Luciferase activity was normalized by fluorescence unit of co-expressed EGFP, which is corresponding to cell viability. No change in fluorescence (that is cell viability) was observed by either mAb. A total of 100-nM DBZ was used as a positive control ($n = 3$–6, $^{**}P < 0.01$). (**b**) Immunoblot analysis of HeLa cells treated with 100 μg/ml of anti-NCT mAbs. (**c**) Effects of A5226A on the endocytosis of the γ-secretase and amyloid precursor protein. HeLa cells were surface labeled with a disulfide-cleavable biotinylation reagent, and then incubated for indicated times. Remaining reagents on the cell surface were stripped with a membrane-impermeant reducing reagent, and the amount of the internalized proteins was analyzed by immunoblotting.

enzyme, while a slight decrease in the levels of PS/γ-secretase complex might additionally contribute to the inhibitory effect. NCT harbors a dual function for the active γ-secretase as a stabilization factor and a regulator for intrinsic enzyme activity (Shirotani *et al.*, 2003; Takasugi *et al.*, 2003; Shah *et al.*, 2005; Chavez-Gutierrez *et al.*, 2008; Dries *et al.*, 2009; Hayashi *et al.*, 2009; Zhao *et al.*, 2010). Therefore, we hypothesized that A5226A inhibits the proteolytic activity by interfering with the interaction between NCT and the substrates. To examine this possibility, we performed co-immunoprecipitation experiments using recombinant NCT and Notch-based substrate, N100 (Figure 5b) (Shah *et al.*, 2005). We observed specific precipitation of NCT with the substrate, which was abolished by SDS-pretreatment of NCT, as previously described (Shah *et al.*, 2005). Addition of A5201A or bovine serum albumin showed no effect on the amount of co-precipitated NCT and N100. In contrast, A5226A reduced the precipitation of the substrate with NCT, suggesting that A5226A interfered with the interaction between NCT and the substrates, thereby reducing the γ-secretase activity.

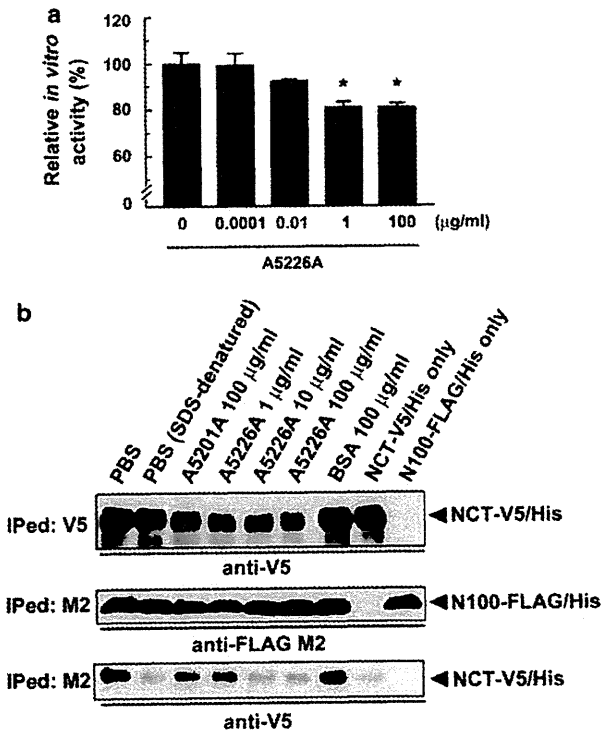

Figure 5 Inhibitory effect of A5226A on γ-secretase activity. (**a**) Effects of anti-NCT mAbs in an *in vitro* γ-secretase assay. Solubilized HeLa cell membranes were co-incubated with recombinant substrate, C100-FmH (Takahashi *et al.*, 2003), in the presence of mAbs at indicated concentration. *De novo* generation levels of amyloid-β peptide were shown ($n=3$, mean ± s.e.m., $^*P<0.05$). (**b**) Effects of anti-NCT mAbs in a binding assay using recombinant NCT and substrate. Co-incubated samples containing N100-FLAG/His and NCT-V5/His with mAbs were immunoprecipitated by antibodies indicated at the left of the panels and analyzed by immunoblot using antibodies below the panels.

Anti-tumor activity of A5226A

Anti-tumor activity of γ-secretase inhibitors has been examined in clinical trials (Pannuti *et al.*, 2010; Yin *et al.*, 2010). The results above that A5226A exhibits an inhibitory activity against γ-secretase, led us to examine the effect on cancer cell proliferation. Among several types of cancer cells, we selected A549 cells derived from non-small cell lung cancer because of its sensitivity to γ-secretase inhibitors (Luistro *et al.*, 2009). Cell viability of A549 cells was reduced by DAPT treatment, whereas that of HeLa cells was not affected. Further, knock-down of endogenous NCT by small interference RNA in A549 cells also resulted in reduced cell viability, suggesting that proliferation of A549 cells is dependent on the γ-secretase activity (Supplementary Figure 2A-C). We next treated A549 and HeLa cells with A5226A. As observed with DAPT, A5226A reduced cell viability of A549 cells but not that of HeLa cells, suggesting that the γ-secretase-dependent proliferation of A549 cells is inhibited by A5226A (Figure 6a). Notably, A5226A treatment further reduced the viability of DAPT-treated A549 cells, suggesting that A5226A is applicable for a combination therapy targeting γ-secretase with small compounds (Figure 6b). Further, we tested the effect of A5226A on the proliferation of lymphoblastic leukemia DND-41 cells carrying activating mutations in *NOTCH1* gene (that is, L1594P and 2444stop) (Weng *et al.*, 2004; Ferrando, 2009; Masuda *et al.*, 2009). Cell survival of DND-41 was sensitive to the treatment by a potent γ-secretase inhibitor dibenzazepine (DBZ) in a similar manner to that of A549 cells (Supplementary Figure 2D). As expected, A5226A treatment, but not control IgG fraction, inhibited the proliferation of DND-41 (Figure 6c) as well as Notch intracellular domain generation (Figure 6d). These data implicated the possibility that γ-secretase-dependent cell survival is also inhibited by A5226A in DND-41. Finally, we examined the anti-tumor activity of A5226A in a xenograft mouse model, in which severe combined immunodeficiency mice were inoculated subcutaneously with DND-41. A5226A, A5201A or control IgG was intraperitoneally administered daily for 4–5 days after inoculation. The size of subcutaneous tumors of the A5226A-treated groups was significantly reduced compared with those of control groups (that is 55.2% reduction in tumor volume at day 38) (Figure 6e). Taken together, we concluded that A5226A functions as an inhibitory mAb for the γ-secretase activity-dependent cancer cell growth *in vivo*.

Discussion

Targeted inhibition of γ-secretase activity has a potential to affect cancer cell proliferation/differentiation and angiogenesis in solid tumors (Ferrando, 2009; Kopan and Ilagan, 2009; Pannuti *et al.*, 2010; Yin *et al.*, 2010). Moreover, the effectiveness of antibodies in treating patients with cancer has been increasingly recognized (Samaranayake *et al.*, 2009; Weiner *et al.*, 2010). In the present study, we have identified a novel

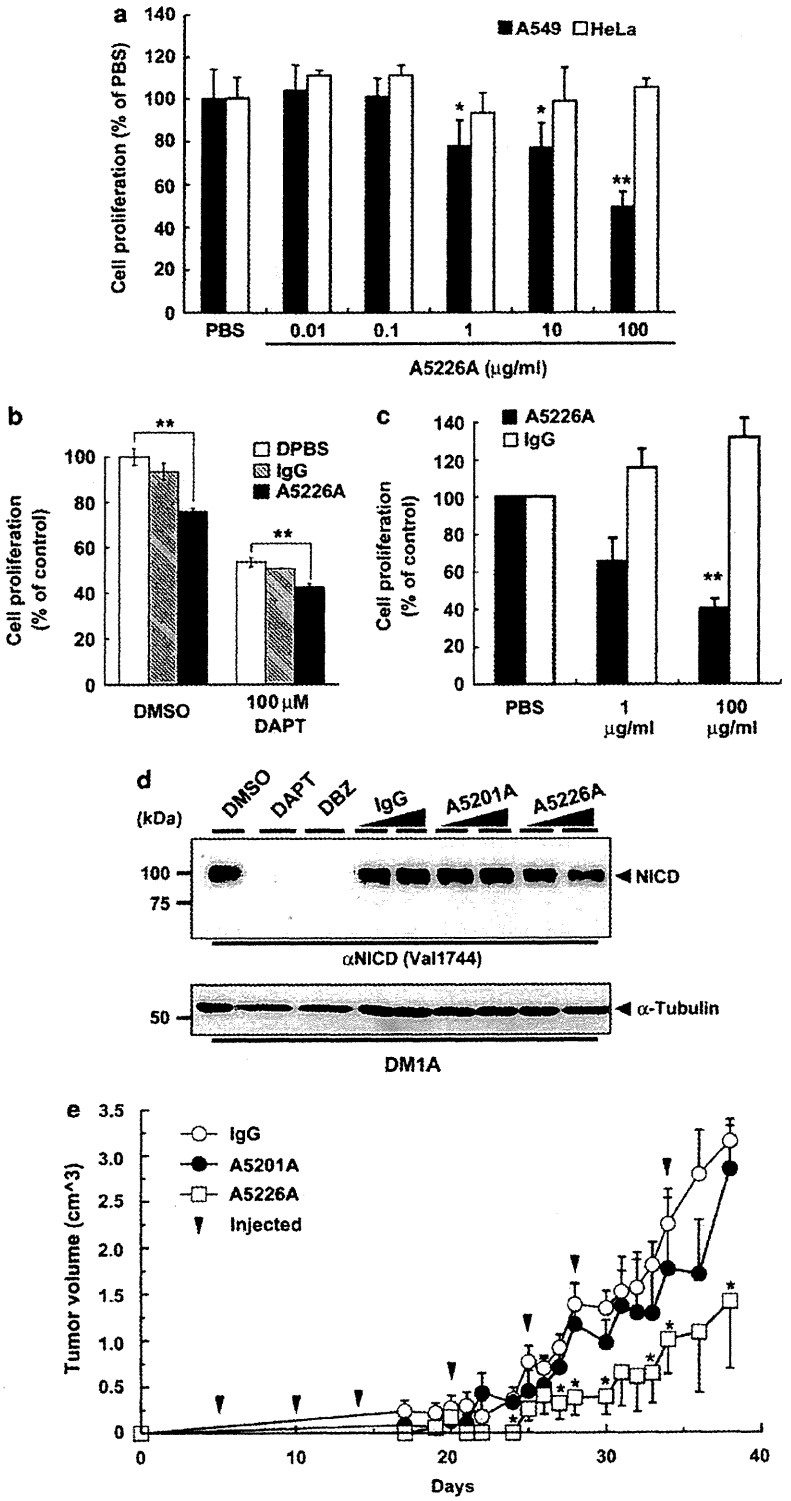

Figure 6 Anti-cancer activity of A5226A. (**a**) Effect of A5226A on the proliferation of A549 cells. Note that γ-secretase activity-dependent cell proliferation of A549 cells was specifically inhibited by A5226A ($n=4$, mean ± s.e.m., $^*P<0.05$, $^{**}P<0.01$). (**b**) Effect of combination treatment of A5226A (100 μg/ml) and DAPT (100 μM) on the proliferation of A549 cells ($n=3$, mean ± s.e.m., $^{**}P<0.01$). (**c**) Effect of A5226A on the proliferation of DND-41 cells ($n=3$, mean ± s.e.m., $^{**}P<0.01$). (**d**) Immunoblot analysis of A5226A-treated DND-41 cells treated with γ-secretase inhibitors (10 μM DAPT and 100 nM DBZ) or mAbs (10 or 100 μg/mL) for 7 days. (**e**) Anti-cancer effects of A5226A on xenograft models of DND-41 cells with concurrent injection of mAbs at a dose of 50 mg/kg/day. Arrowheads denote the dates of injection. Data represent the mean tumor volume (cm^3) ± s.d. ($n=3$, $^*P<0.05$).

antibody A5226A against NCT ECD generated by a novel budded baculovirus immunization technology. Biochemical and cell biological analyses showed that A5226A recognizes the active γ-secretase complex containing mature NCT located at CTB-positive microdomain on the plasma membrane. Moreover, A5226A inhibited the γ-secretase activity by perturbing the NCT/substrate interaction, and also showed the inhibitory activity for proliferation of cancer cells both *in vitro* and *in vivo*. These data provided us with the compelling evidence that NCT is a molecular target for the modulation of γ-secretase activity, and that the anti-NCT mAb A5226A is applicable to cancer immunotherapy targeting γ-secretase and Notch.

It has been reported that functionally active, properly folded recombinant proteins can be displayed on baculoviral virion membranes released from infected insect cells (Masuda *et al.*, 2003; Urano *et al.*, 2003; Hayashi *et al.*, 2004; Saitoh *et al.*, 2006). Thus, utilizing budded baculovirus as immunogen is a versatile approach to generate mAbs against membrane proteins of interest. Using this technology, we have generated A5201A and A5226A that specifically interact with recombinant NCT ECD with different binding properties. Using deletion and swap mutants of NCT, we found that the epitope of A5226A locates around the residues R391 in human NCT ECD. To gain a structural insight on the significance of R391, we built a homology model of NCT ECD using the structure of transferrin receptor (TfR; PDB ID: 1CX8) as a template (Supplementary Figure 3) (Lawrence *et al.*, 1999). In this model, E333 and the DYIGS motif that are required for the folding and activity of NCT (Yu *et al.*, 2000; Shirotani *et al.*, 2004; Shah *et al.*, 2005; Chavez-Gutierrez *et al.*, 2008; Dries *et al.*, 2009) are situated at the back of a deep channel made by the peptidase-like domain and the apical domain. They correspond to, or lie close to, the active site residues in homologous aminopeptidases and may constitute a putative substrate binding pocket (Shah *et al.*, 2005). Intriguingly, R391 is located in a loop that constitutes an entrance of this channel, suggesting that the binding of A5226A may obstruct the access of substrates. Although the precise function of NCT still remains controversial (Shah *et al.*, 2005; Chavez-Gutierrez *et al.*, 2008; Dries *et al.*, 2009; Hayashi *et al.*, 2009; Zhao *et al.*, 2010), the neutralizing mAb A5226A inhibited the binding between NCT and substrates *in vitro*, supporting the notion that one of the NCT functions is a substrate receptor. Also, we observed that A5226A treatment slightly decreased the levels of PS1 fragments; a slight reduction in the active enzyme might have potentiated the inhibitory effect of A5226A *in vivo*. Taken together, as the major mechanism of action of A5226A, one can speculate that the binding of mAb to NCT located on the cell surface might mask a region around E333 and the DYIGS motif and thereby inhibit the substrate recognition by NCT. Further structural studies at an atomic level using X-ray crystallography, nuclear magnetic resonance or other techniques would help us to understand the mode of action of A5226A.

To date, the precise localization of the endogenous γ-secretase complex remains unclear. By immunocytochemical analyses, we found that A5226A-positive endogenous NCT is co-localized with CTB-positive patches on the cell surface. CTB is a ligand for GM1 ganglioside that is enriched on the lipid raft microdomain (Boesze-Battaglia, 2006). In accordance with our results, several lines of evidence indicate that γ-secretase activity is biochemically detected in lipid raft fractions (Urano *et al.*, 2005; Vetrivel and Thinakaran, 2010), suggesting that A5226A-positive patches represent the localization of the endogenous active γ-secretase complex at the cell surface. Recently, biochemical co-purification of tetraspanins (that is CD9 and CD81) with active γ-secretase complex was reported (Wakabayashi *et al.*, 2009), which form cholesterol-rich lipid raft-like microdomains termed tetraspanin-enriched microdomains. However, CTB-positive patches were not co-localized with CD9 nor CD81 on NKO/hNCT cell surface (Supplementary Figure 4), suggesting that A5226A-positive patches are distinct from tetraspanin-enriched microdomains containing CD9 or CD81. However, several tetraspanins form different microdomains in a cell-type or subcellular localization-specific manner. In particular, TSPAN5 and TSPAN33 are implicated in γ-secretase cleavage of Notch (Dunn *et al.*, 2010). It would be of interest to examine if CTB- and A5226A-positive patches contain tetraspanins. Further molecular and biochemical analyses would be needed to clarify the nature of CTB- and A5226A-patches on the cell surface.

Chemical biology studies revealed that all γ-secretase inhibitors investigated so far target PS (Tomita, 2009). Our results clearly indicate that targeting NCT function by A5226A is effective against cancer cell growth *in vitro* as well as *in vivo*. Moreover, a combination approach with DAPT increased the efficacy, suggesting that targeting NCT ECD is a novel and versatile approach against γ-secretase activity-dependent cancers. Supporting this notion, it has been recently reported that the expression levels of NCT were upregulated in breast cancer, and that a loss-of-function of NCT decreased the cell proliferation of breast cancer cells (Filipovic *et al.*, 2011). However, a remaining issue on targeting γ-secretase activity is the adverse effects by total Notch signaling inhibition (Tomita, 2009; De Strooper *et al.*, 2010). In this context, targeted inhibition of Notch1 or Notch2 by specific mAbs showed low toxicity (Wu *et al.*, 2010), supporting the notion that mechanism-based adverse effects associated with Notch signaling inhibition can be avoided by using a substrate-specific inhibition. Although A5226A showed similar levels of inhibition against amyloid precursor protein and Notch cleavages in a cell-based assay, it remains to be determined whether A5226A inhibits all four Notch family members and what other substrates might be preferentially inhibited. Intriguingly, some point mutations at NCT ECD affected the γ-secretase activity in a substrate-specific manner (Chavez-Gutierrez *et al.*, 2008), suggesting that NCT ECD is involved in the substrate selectivity of γ-secretase. Thus, substrate-

specific inhibitory mAbs might be obtained by targeting NCT ECD. In addition, subcellular localization of the substrates might also affect the substrate preference of γ-secretase (Vetrivel and Thinakaran, 2010). Understanding possible substrates within the A5226A-positive patches on the cell surface will be of considerable interest. Therapeutic mAbs provide clinical benefit by target specificity, low toxicity and longer half-lives *in vivo*. Importantly, mAbs can be engineered on a more rational basis to enhance the efficacy and the specificity (Samaranayake *et al.*, 2009; Weiner *et al.*, 2010). Nevertheless, more in depth understandings of the complex biology of γ-secretase regarding its substrate selectivity will be needed to predict liabilities of γ-secretase inhibitors and inhibitory mAbs such as A5226A.

In summary, we have established anti-NCT mAb A5226A that neutralizes the γ-secretase activity, thereby affecting cancer cell proliferation *in vivo*. Development of therapeutic mAbs will not only provide clinical benefits to patients but also lead to discoveries of functions of unknown cell surface antigens (Samaranayake *et al.*, 2009; Weiner *et al.*, 2010). Our results support the notion that one of the NCT functions is a substrate binding, which was inhibited by A5226A, at GM1-positive domain on the cell surface. Importantly, to our knowledge, A5226A is the first mAb that regulates the proteolytic activity of the intramembrane proteases, which execute emerging biological and pathological functions, by the inhibition of substrate recognition. Nevertheless, our present study also suggests that small molecules or proteins that regulate the NCT activity might provide a novel therapeutic strategy for modulating the γ-secretase activity against cancers.

Materials and methods

Immunization, generation of hybridoma, screenings, purification of ascites and characterization

Construction of expression plasmid, cell culture, transfection/infection and immunological methods are shown in Supplementary Methods. For generation of mAbs using NCT-expressing budded baculovirus as an immunogen, transgenic mice expressing gp64, a major viral envelope protein, were immunized five times (Saitoh *et al.*, 2007). Hybridoma cells were generated by a standard polyethylene glycol-mediated method using splenocytes and NS-1 myeloma cells. Hybridoma cells were maintained in RPMI-1640 medium containing 15% (v/v) fetal bovine serum, penicillin/streptomycin, 2 mM of L-glutamine (Invitrogen, Carlsbad, CA, USA), 1 mM of sodium pyruvate (SIGMA, St Louis, MO, USA) and 45 μg/ml of gentamicin (Schering-Plough, Kenilworth, NJ, USA). Enzyme-linked immunosorbent assay screenings were performed using mock or NCT-expressing budded baculovirus as a capture antigen. For the preparation of ascites, hybridoma cells ($1–3 \times 10^7$ cells) were injected intraperitoneally to 6-week-old male BALB/c mice, which were treated with pristane (SIGMA) 3–7 days before the injection. After 10–14 days, the ascites were collected and purified with MAbTrap kit (GE Healthcare, Piscataway, NJ, USA). Purified ascites were stored at −80 °C until used. For Scatchard plot, 10 μg/ml of mAbs were incubated with 0, 0.19, 0.38, 0.75 or 1.5 μM of NCT ECD to form antibody/antigen complex and were applied to NCT ECD-coated plates. Subsequently, anti-mouse IgG antibody conjugated with horseradish peroxidase was incubated, and the binding of free mAb was quantitated by measuring OD450 using peroxidase substrate.

NCT-substrate binding assay

Microsome fraction was obtained from infected Sf9 cells expressing NCT-V5/His or N100-FLAG/His. After solubilization by 1% 3-[(3-cholamidopropyl)dimethylammonio]-2-hydroxypropanesulfonate (CHAPSO), the lysates were mixed with or without antibodies, and pulled down by anti-V5 or FLAG antibody-conjugated agarose beads (SIGMA). The precipitated proteins were eluted by sample buffer and analyzed by immunoblot.

Cell viability assay

Cells were plated in 96-well plates ($2.5–5 \times 10^3$ cells per well) 24 h before the addition of designated concentrations of γ-secretase inhibitors or mAbs. Equal concentration of the vehicle carrier (dimethyl sulfoxide or phosphate-buffered saline, respectively) was always present in the control wells. After incubation for indicated time, 20 μl of 2.5 mg/ml of 3-(4,5-dimethylthiazol-2-yl)-2,5-diphenyltetrazolium bromide (final concentration: 400 μg/ml) or 10 μl of Alamar Blue (Serotec, Oxford, UK) was added to each well and incubated for 3–4 h at 37 degrees. In the case of 3-(4,5-dimethylthiazol-2-yl)-2,5-diphenyltetrazolium bromide, solubilization of the precipitate was performed with 200 μl of stop solution (10% (w/v) SDS and 0.01 M HCl). Cell viability was calculated from absorption or fluorescence values for 3-(4,5-dimethylthiazol-2-yl)-2,5-diphenyltetrazolium bromide or Alamar Blue, respectively.

In vivo *xenograft assay*

Severe combined immunodeficiency mice (C.B-17/Icr-scid/scid Jcl; 6-weeks-old female) were purchased from CLEA Japan (Tokyo, Japan) and maintained under specific pathogen-free conditions. All experimental procedures were performed in accordance with the guidelines for animal experiments of the University of Tokyo. For xenograft mouse model (Masuda *et al.*, 2009), severe combined immunodeficiency mice at 6–8 weeks of age were inoculated subcutaneously in the right flank with 3×10^7 cells in 300 μl of phosphate buffered saline, and were randomly assigned to control or mAb-treated groups the day after tumor inoculation. The antibodies were administered intraperitoneally every 4–5 days for at least 30 days at a dose of 50 mg/kg/day. Tumor size was measured at the greatest length and width. The volume was calculated as $1/2 \times (\text{tumor length}) \times (\text{tumor width})^2$.

Conflict of interest

The authors declare no conflict of interest.

Acknowledgements

We are grateful to Drs T Fukuyama, S Yokoshima (The University of Tokyo), C Haass (Ludwig-Maximilians-University München), H Natsugari (Teikyo University), R Kopan (Washington University in St Louis), G Thinakaran (The University of Chicago), M Vooijs (University Medical Center Utrecht Cancer Center) and G Yu (The University of Texas

Southwestern Medical Center) for valuable reagents and our current and previous laboratory members for helpful discussions. We also would like to thank Keiko Tamura-Kawakami and Maiko Nampo for their excellent technical support. This work is supported in part by Grants-in-Aid for Young Scientists (S) (for TT) from Japan Society for the Promotion of Science (JSPS), by the Program for Promotion of Fundamental Studies in Health Sciences of the National Institute of Biomedical Innovation (for TT, TI), Scientific Research on Priority Areas 'Research on Pathomechanisms of Brain Disorders' from the Ministry of Education, Culture, Sports, Science and Technology (MEXT) (for TT, TI), by Targeted Proteins Research Program grant from the MEXT (for TT, TI, JT), by Core Research for Evolutional Science and Technology grant from the MEXT (for TT, TI), Japan. IH and ST were research fellows of JSPS.

References

Boesze-Battaglia K. (2006). Isolation of membrane rafts and signaling complexes. *Methods Mol Biol* **332**: 169–179.

Chavez-Gutierrez L, Tolia A, Maes E, Li T, Wong PC, de Strooper B. (2008). Glu(332) in the Nicastrin ectodomain is essential for γ-secretase complex maturation but not for its activity. *J Biol Chem* **283**: 20096–20105.

De Strooper B, Vassar R, Golde T. (2010). The secretases: enzymes with therapeutic potential in Alzheimer disease. *Nat Rev Neurol* **6**: 99–107.

Dries DR, Shah S, Han YH, Yu C, Yu S, Shearman MS *et al.* (2009). Glu-333 of nicastrin directly participates in γ-secretase activity. *J Biol Chem* **284**: 29714–29724.

Dunn CD, Sulis ML, Ferrando AA, Greenwald I. (2010). A conserved tetraspanin subfamily promotes Notch signaling in *Caenorhabditis elegans* and in human cells. *Proc Natl Acad Sci USA* **107**: 5907–5912.

Esler WP, Kimberly WT, Ostaszewski BL, Ye W, Diehl TS, Selkoe DJ *et al.* (2002). Activity-dependent isolation of the presenilin-γ-secretase complex reveals nicastrin and a γ substrate. *Proc Natl Acad Sci USA* **99**: 2720–2725.

Fan X, Matsui W, Khaki L, Stearns D, Chun J, Li YM *et al.* (2006). Notch pathway inhibition depletes stem-like cells and blocks engraftment in embryonal brain tumors. *Cancer Res* **66**: 7445–7452.

Ferrando AA. (2009). The role of NOTCH1 signaling in T-ALL. *Hematology (Am Soc Hematol Educ Program)* **2009**: 353–361.

Filipovic A, Gronau JH, Green AR, Wang J, Vallath S, Shao D *et al.* (2011). Biological and clinical implications of nicastrin expression in invasive breast cancer. *Breast Cancer Res Treat* **125**: 43–53.

Hayashi I, Takatori S, Urano Y, Iwanari H, Isoo N, Osawa S *et al.* (2009). Single chain variable fragment against nicastrin inhibits the γ-secretase activity. *J Biol Chem* **284**: 27838–27847.

Hayashi I, Urano Y, Fukuda R, Isoo N, Kodama T, Hamakubo T *et al.* (2004). Selective reconstitution and recovery of functional γ-secretase complex on budded baculovirus particles. *J Biol Chem* **279**: 38040–38046.

Imamura Y, Watanabe N, Umezawa N, Iwatsubo T, Kato N, Tomita T *et al.* (2009). Inhibition of γ-secretase activity by helical β-peptide foldamers. *J Am Chem Soc* **131**: 7353–7359.

Kaether C, Lammich S, Edbauer D, Ertl M, Rietdorf J, Capell A *et al.* (2002). Presenilin-1 affects trafficking and processing of βAPP and is targeted in a complex with nicastrin to the plasma membrane. *J Cell Biol* **158**: 551–561.

Kimura K, Satoh K, Kanno A, Hamada S, Hirota M, Endoh M *et al.* (2007). Activation of Notch signaling in tumorigenesis of experimental pancreatic cancer induced by dimethylbenzanthracene in mice. *Cancer Sci* **98**: 155–162.

Kopan R, Ilagan MX. (2009). The canonical Notch signaling pathway: unfolding the activation mechanism. *Cell* **137**: 216–233.

Lawrence CM, Ray S, Babyonyshev M, Galluser R, Borhani DW, Harrison SC. (1999). Crystal structure of the ectodomain of human transferrin receptor. *Science* **286**: 779–782.

LaVoie MJ, Fraering PC, Ostaszewski BL, Ye W, Kimberly WT, Wolfe MS *et al.* (2003). Assembly of the γ-secretase complex involves early formation of an intermediate subcomplex of Aph-1 and nicastrin. *J Biol Chem* **278**: 37213–37222.

Li T, Ma G, Cai H, Price DL, Wong PC. (2003). Nicastrin is required for assembly of presenilin/γ-secretase complexes to mediate Notch signaling and for processing and trafficking of β-amyloid precursor protein in mammals. *J Neurosci* **23**: 3272–3277.

Luistro L, He W, Smith M, Packman K, Vilenchik M, Carvajal D *et al.* (2009). Preclinical profile of a potent γ-secretase inhibitor targeting notch signaling with *in vivo* efficacy and pharmacodynamic properties. *Cancer Res* **69**: 7672–7680.

Masuda K, Itoh H, Sakihama T, Akiyama C, Takahashi K, Fukuda R *et al.* (2003). A combinatorial G protein-coupled receptor reconstitution system on budded baculovirus. Evidence for Galpha and Galphao coupling to a human leukotriene B4 receptor. *J Biol Chem* **278**: 24552–24562.

Masuda S, Kumano K, Suzuki T, Tomita T, Iwatsubo T, Natsugari H *et al.* (2009). Dual antitumor mechanisms of Notch signaling inhibitor in a T-cell acute lymphoblastic leukemia xenograft model. *Cancer Sci* **100**: 2444–2450.

Osipo C, Patel P, Rizzo P, Clementz AG, Hao L, Golde TE *et al.* (2008). ErbB-2 inhibition activates Notch-1 and sensitizes breast cancer cells to a γ-secretase inhibitor. *Oncogene* **27**: 5019–5032.

Pannuti A, Foreman K, Rizzo P, Osipo C, Golde T, Osborne B *et al.* (2010). Targeting Notch to target cancer stem cells. *Clin Cancer Res* **16**: 3141–3152.

Saitoh R, Ohtomo T, Ito Y, Nezu J, Kimura N, Funahashi S *et al.* (2006). Recovery of functional peptide transporter PepT1 in budded baculovirus fraction. *Protein Expr Purif* **46**: 130–135.

Saitoh R, Ohtomo T, Yamada Y, Kamada N, Nezu J, Kimura N *et al.* (2007). Viral envelope protein gp64 transgenic mouse facilitates the generation of monoclonal antibodies against exogenous membrane proteins displayed on baculovirus. *J Immunol Methods* **322**: 104–117.

Samaranayake H, Wirth T, Schenkwein D, Raty JK, Yla-Herttuala S. (2009). Challenges in monoclonal antibody-based therapies. *Ann Med* **41**: 322–331.

Shah S, Lee SF, Tabuchi K, Hao YH, Yu C, LaPlant Q *et al.* (2005). Nicastrin functions as a γ-secretase-substrate receptor. *Cell* **122**: 435–447.

Shirotani K, Edbauer D, Capell A, Schmitz J, Steiner H, Haass C. (2003). γ-secretase activity is associated with a conformational change of nicastrin. *J Biol Chem* **278**: 16474–16477.

Shirotani K, Edbauer D, Kostka M, Steiner H, Haass C. (2004). Immature nicastrin stabilizes APH-1 independent of PEN-2 and presenilin: identification of nicastrin mutants that selectively interact with APH-1. *J Neurochem* **89**: 1520–1527.

Takasugi N, Tomita T, Hayashi I, Tsuruoka M, Niimura M, Takahashi Y *et al.* (2003). The role of presenilin cofactors in the γ-secretase complex. *Nature* **422**: 438–441.

Takahashi Y, Hayashi I, Tominari Y, Rikimaru K, Morohashi Y, Kan T *et al.* (2003). Sulindac sulfide is a noncompetitive γ-secretase inhibitor that preferentially reduces Aβ42 generation. *J Biol Chem* **278**: 18664–18670.

Tarassishin L, Yin YI, Bassit B, Li YM. (2004). Processing of Notch and amyloid precursor protein by γ-secretase is spatially distinct. *Proc Natl Acad Sci USA* **101**: 17050–17055.

Tomita T, Katayama R, Takikawa R, Iwatsubo T. (2002). Complex *N*-glycosylated form of nicastrin is stabilized and selectively bound to presenilin fragments. *FEBS Lett* **520**: 117–121.

Tomita T. (2009). Secretase inhibitors and modulators for Alzheimer's disease treatment. *Expert Rev Neurother* **9**: 661–679.

Urano Y, Hayashi I, Isoo N, Reid PC, Shibasaki Y, Noguchi N *et al.* (2005). Association of active γ-secretase complex with lipid rafts. *J Lipid Res* **46**: 904–912.

Urano Y, Yamaguchi M, Fukuda R, Masuda K, Takahashi K, Uchiyama Y *et al.* (2003). A novel method for viral display of ER membrane proteins on budded baculovirus. *Biochem Biophys Res Commun* **308**: 191–196.

Vetrivel KS, Thinakaran G. (2010). Membrane rafts in Alzheimer's disease β-amyloid production. *Biochim Biophys Acta* **1801**: 860–867.

Wakabayashi T, Craessaerts K, Bammens L, Bentahir M, Borgions F, Herdewijn P *et al.* (2009). Analysis of the γ-secretase interactome and validation of its association with tetraspanin-enriched microdomains. *Nat Cell Biol* **11**: 1340–1346.

Weiner LM, Surana R, Wang S. (2010). Monoclonal antibodies: versatile platforms for cancer immunotherapy. *Nat Rev Immunol* **10**: 317–327.

Weng AP, Ferrando AA, Lee W, Morris JPt, Silverman LB, Sanchez-Irizarry C *et al.* (2004). Activating mutations of NOTCH1 in human T cell acute lymphoblastic leukemia. *Science* **306**: 269–271.

Wu Y, Cain-Hom C, Choy L, Hagenbeek TJ, de Leon GP, Chen Y *et al.* (2010). Therapeutic antibody targeting of individual Notch receptors. *Nature* **464**: 1052–1057.

Yin L, Velazquez OC, Liu ZJ. (2010). Notch signaling: emerging molecular targets for cancer therapy. *Biochem Pharmacol* **80**: 690–701.

Yu G, Nishimura M, Arawaka S, Levitan D, Zhang L, Tandon A *et al.* (2000). Nicastrin modulates presenilin-mediated *notch/glp-1* signal transduction and βAPP processing. *Nature* **407**: 48–54.

van Es JH, Clevers H. (2005). Notch and Wnt inhibitors as potential new drugs for intestinal neoplastic disease. *Trends Mol Med* **11**: 496–502.

van Tetering G, van Diest P, Verlaan I, van der Wall E, Kopan R, Vooijs M. (2009). Metalloprotease ADAM10 is required for Notch1 site 2 cleavage. *J Biol Chem* **284**: 31018–31027.

Zhao G, Liu Z, Ilagan MX, Kopan R. (2010). γ-secretase composed of PS1/Pen2/Aph1a can cleave notch and amyloid precursor protein in the absence of nicastrin. *J Neurosci* **30**: 1648–1656.

Supplementary Information accompanies the paper on the Oncogene website (http://www.nature.com/onc)

The FASEB Journal • Research Communication

An alternative metabolic pathway of amyloid precursor protein C-terminal fragments *via* cathepsin B in a human neuroglioma model

Masashi Asai,[*,†,1,2] Sosuke Yagishita,[‡,2,3] Nobuhisa Iwata,[†,§] Takaomi C. Saido,[†] Shoichi Ishiura,[‡] and Kei Maruyama[*]

[*]Department of Pharmacology, Faculty of Medicine, Saitama Medical University, Saitama, Japan; [†]Laboratory for Proteolytic Neuroscience, RIKEN Brain Science Institute, Saitama, Japan; [‡]Department of Life Sciences, Graduate School of Arts and Sciences, The University of Tokyo, Tokyo, Japan; and [§]Graduate School of Biomedical Sciences, Nagasaki University, Nagasaki, Japan

ABSTRACT **γ-Secretase catalyzes the cleavage of the intramembrane region of the Alzheimer amyloid precursor protein (APP), generating p3, amyloid-β peptide (Aβ), and the APP intracellular domain (AICD). Although a γ-secretase inhibitor has been shown to cause an accumulation of the APP C-terminal fragments (CTFs) α and β and to decrease levels of p3 or Aβ and AICD, we found that treatment with a lysosomotropic weak base, such as chloroquine or ammonium chloride, caused simultaneous accumulation of both CTFs and AICD, suggesting that lysosomal proteases are also involved in processing of APP. This observation was reinforced by the results that cysteine protease inhibitor E-64d and cathepsin B specific inhibitor CA-074Me caused the accumulation of both CTFs and AICD with no change in known secretase activities. γ-Secretase preferentially cleaved phosphorylated CTFs to produce Aβ, but cathepsin B degraded CTFs regardless of phosphorylation. Our results suggest that cathepsin B plays novel roles in the metabolism of APP and that an inhibition of APP phosphorylation is an attractive therapeutic target for Alzheimer's disease.—Asai, M., Yagishita, S., Iwata, N., Saido, T. C., Ishiura, S., Maruyama, K. An alternative metabolic pathway of amyloid precursor protein C-terminal fragments *via* cathepsin B in a human neuroglioma model. *FASEB J.* 25, 3720–3730 (2011). www.fasebj.org**

Key Words: Alzheimer's disease · CA-074Me · γ-secretase · phosphorylation

AMYLOID PRECURSOR PROTEIN (APP) is a type I integral membrane glycoprotein with a single membrane-spanning domain, a large ectoplasmic N-terminal region, and a shorter cytoplasmic C-terminal region (1–3). An understanding of APP metabolism is physiologically and clinically important because APP is a stepwise substrate for β- and γ-secretases in the production of the neurotoxic amyloid-β peptide (Aβ; Aβ40 or Aβ42; refs. 1–4). Thus, β- and γ-secretase inhibitors are pharmacological targets for the treatment or prevention of Alzheimer's disease (AD; refs. 4, 5).

Proteolytic processing of APP has been extensively studied, and two major processing pathways have been described. Initially, α- or β-secretase cleaves APP to produce a secreted N-terminal soluble extracellular fragment of APP (sAPPα or sAPPβ) and membrane-bound C-terminal fragments of APP (CTFα or CTFβ). Sequentially, γ-secretase catalyzes the intramembrane proteolysis of CTFs to produce p3, Aβ, and APP intracellular domain (AICD; refs. 1–4).

Numerous γ-secretase inhibitors have been developed (2, 4, 5), and treatment with a γ-secretase inhibitor causes accumulation of substrates, such as CTFs, and suppression of the production of Aβ and AICD *in vivo* or *in vitro* (6–9). This quantitative balance of CTFs, Aβ, and AICD seems to be dependent on γ-secretase, which is an enzymatic multiprotein complex containing presenilin (PS; either PS1 or PS2) as the active core. However, it has been reported that both CTFs and AICD simultaneously accumulated under treatment with lysosomotropic weak bases, such as chloroquine or ammonium chloride (NH_4Cl; refs. 10, 11). It is highly unlikely that alkalization of the endosome-lysosome system causes γ-secretase dysfunction because γ-secretase can cleave other substrates, such as Notch, and can produce intracellular fragments in the presence of these lysosomal inhibitors. In other words, the accumulation of both products and substrates of γ-secretase is indicative of the presence of proteases other than γ-secretase for the processing of CTFs and AICD.

To identify CTF- and AICD-processing enzymes, we analyzed APP metabolism using a pharmacological

[1] Correspondence: Department of Pharmacology, Faculty of Medicine, Saitama Medical University, 38 Moro-hongo, Moroyama-machi, Iruma-gun, Saitama 350-0495, Japan. E-mail: asai@saitama-med.ac.jp

[2] These authors contributed equally to this work.

[3] Current address: Laboratory for Alzheimer's Disease, RIKEN Brain Science Institute, Saitama, Japan.

doi: 10.1096/fj.11-182154

This article includes supplemental data. Please visit *http://www.fasebj.org* to obtain this information.

0892-6638/11/0025-3720 © FASEB

approach in a human neuroglioma model. We found that cysteine protease inhibitor E-64d (12) and cathepsin B-specific inhibitor CA-074Me (12–15) could cause the accumulation of both CTFs and AICD with no change in α-, β-, and γ-secretase activities. Moreover, we found that γ-secretase prefers phosphorylated CTFs on Thr668 (at a position corresponding to the APP_{695} isoform), whereas cathepsin B catalyzed degradation of CTFs regardless of phosphorylation. Altogether, our results suggest that cathepsin B plays novel roles in the metabolism of the APP C-terminal region and that inhibition of APP phosphorylation is an attractive therapeutic target for AD.

MATERIALS AND METHODS

Reagents

CA-074 (also known as cathepsin B inhibitor III; [L-3-*trans*-(propylcarbamoyl)oxirane-2-carbonyl]-L-isoleucyl-L-proline), CA-074Me (also known as cathepsin B inhibitor IV; [L-3-*trans*-(propylcarbamoyl)oxirane-2-carbonyl]-L-isoleucyl-L-proline methyl ester), E-64d [(L-3-*trans*-ethoxycarbonyloxirane-2-carbonyl)-L-leucine (3-methylbutyl) amide], lactacystine ([*N*-acetyl-*S*-{(2*R*,3*S*,4*R*)-3-hydroxy-2-[(1*S*)-1-hydroxy-2-methylpropyl]-4-methyl-5-oxo-2-pyrrolidinecarbonyl}-L-cysteine), DAPT [also known as γ-secretase inhibitor IX; (3,5-difluorophenylacetyl)-L-alanyl-L-2-phenylglycine *t*-butyl ester], and L-685,458 (also known as γ-secretase inhibitor X; [(2*R*,4*R*,5*S*)-2-benzyl-5-(*t*-butyloxycarbonylamino)-4-hydroxy-6-phenylhexanoyl]-L-leucyl-L-phenylalanine amide) were purchased from the Peptide Institute (Osaka, Japan). β-Secretase inhibitor IV (*N*-[(1*S*, 2*R*)-1-benzyl-3-(cyclopropylamino)-2-hydroxypropyl]-5-[methyl(methylsulfonyl)amino-*N*'-[(1*R*)-1-phenylethyl]isophthalamide), compound E (also known as γ-secretase inhibitor XXI; (*S*,*S*)-2-[2-(3,5-difluorophenyl)-acetylamino]-*N*-(1-methyl-2-oxo-5-phenyl-2,3-dihydro-1H-benzo[e] [1,4]diazepin-3-yl)-propionamide), and cathepsin G inhibitor I ([2-[3-[(1-benzoylpiperidin-4-yl)-methylcarbamoyl] naphthalen-2-yl]-1-naphthalen-1-yl-2-oxoethyl]phosphonic acid) were purchased from Merck KGaA (Darmstadt, Germany). Pepstatin A, chloroquine, and NH_4Cl were obtained from Sigma-Aldrich Co. (St. Louis, MO, USA). Chloroquine was dissolved in sterilized PBS, and all other powdered reagents were dissolved in sterilized dimethyl sulfoxide (DMSO) and added into the cell culture medium to yield 0.2% DMSO as a final concentration.

Cell culture

A murine neuroblastoma Neuro2a (N2a) cell line ($mNotch^{\Delta E}$-N2a cells) stably expressing both mouse Notch-deleted extracellular domain with myc tag ($mNotch^{\Delta E}$) and enhanced green fluorescent protein (16), a human neuroglioma H4 cell line stably expressing human APP_{695} with the Swedish mutation (APP_{NL}-H4 cells) (17) or stably expressing human APP_{695} with the Swedish mutation and a point mutation at a phosphorylation site [Thr to Ala on 668 (APP_{695} numbering); APP_{NL_TA}-H4 cells], and mouse embryonic fibroblast cells with deficiencies of both *PS1* and *PS2* genes ($PS1^{-/-}PS2^{-/-}$ cells) (18) were cultured in DMEM (Invitrogen, Carlsbad, CA, USA) at 37°C in 5% CO_2. The DMEM was supplemented with 10% FBS (Invitrogen), 100 U/ml penicillin, and 100 μg/ml streptomycin (Invitrogen). In addition, G418 (Merck) was supplemented for $mNotch^{\Delta E}$-N2a cells (160 μg/ml) and $PS1^{-/-}PS2^{-/-}$ cells (200 μg/ml), and hygromycin B (Wako Pure Chemicals Industries, Osaka, Japan) was supplemented for APP_{NL}-H4 cells (150 μg/ml) and APP_{NL_TA}-H4 cells (225 μg/ml). After passage by trypsinization, cells were grown for 24–36 h and then treated with reagents: CA-074Me (0.1, 1, or 10 μM), pepstatin A (10 μM), cathepsin G inhibitor I (10 μM), E-64d (10 μM), compound E (1 μM), DAPT (1 μM), L-685,458 (1 μM), β-secretase inhibitor IV (1 μM), lactacystin (1 μM), chloroquine (1 μM), or NH_4Cl (1 mM), for the indicated time.

Sample preparation for Western blot analysis

Cells treated with reagents were harvested and lysed in a buffer containing 10 mM HEPES (pH 7.4), 150 mM NaCl, 0.5% Triton X-100, and protease inhibitor cocktail (Roche Diagnostics, Mannheim, Germany) on ice. The cell lysate was freeze-thawed at three 20-min intervals and centrifuged at 13,000 *g* for 15 min at 4°C. The supernatant protein concentrations were determined using a BCA protein assay kit (Pierce Biotechnology, Rockford, IL, USA). sAPP secreted into the conditioned medium was precipitated with heparin agarose resin (Pierce Biotechnology), as described previously (16).

Western blot analysis

Equal amounts of proteins from the cell lysates or sAPP collected from the equal volumes of the conditioned medium were subjected to SDS-PAGE, and proteins in the gels were transferred to PVDF membranes (Hybond-P; GE Healthcare, Little Chalfont, UK) or nitrocellulose transfer membranes (Protran; Whatman, Dassel, Germany). The membranes were probed with an appropriate primary antibody and then reacted with an appropriate secondary antibody, specifically horseradish peroxidase-conjugated anti-mouse or anti-rabbit IgG (GE Healthcare). The protein band was visualized using an enhanced chemiluminescence (ECL) detection method (GE Healthcare), and band intensity was analyzed with a densitometer (LAS-4000; GE Healthcare), using Science Laboratory 2001 Image Gauge software (GE Healthcare).

Monoclonal antibody 2B3 (Immuno-Biological Laboratories, Gunma, Japan), which recognizes amino acid residues at the C terminus of human sAPPα, was used at a concentration of 2 μg/ml to detect sAPPα (anti-sAPPα antibody). Polyclonal anti-$sAPP\beta_{NL}$ antibody was used at a concentration of 1:1000 to detect $sAPP\beta_{NL}$ (APP with Swedish mutation), as described previously (17). Monoclonal antibody 82E1 (Immuno-Biological Laboratories), which recognizes amino acid residues 1–16 of the human Aβ sequence, was used at a concentration of 1 μg/ml to detect Aβ (anti-Aβ antibody). Polyclonal anti-APP antibody (catalog no. A8717; Sigma-Aldrich), which recognizes amino acid residues 676–695 at the C terminus of the APP_{695} isoform, was used at a concentration of 1:15,000 to detect full-length APP (FL-APP), CTFs, and AICD (anti-APP antibody). Polyclonal anti-phosphorylated APP antibody (Cell Signaling Technology, Danvers, MA, USA), which recognizes the phosphorylation of Thr668, was used at a concentration of 1:1000. Monoclonal antibody AC-74 (Sigma-Aldrich), which recognizes amino acid residues at the N-terminal end of β-actin, was used at a concentration of 1:5000. Monoclonal antibody 9B11 (Cell Signaling Technology), which recognizes the myc epitope tag corresponding to amino acid residues 410–419 of human c-Myc, was used at a concentration of 1:1000.

Cell-free assay

The microsomal fraction was isolated from APP_{NL}-H4 cells, as described previously (8). Briefly, harvested APP_{NL}-H4 cells

were homogenized in buffer A (20 mM PIPES, pH 7.0; 140 mM KCl; 0.25 M sucrose; and 5 mM EGTA), and the homogenates were then centrifuged at 800 *g* for 10 min to remove nuclei and cell debris. The resultant supernatants were centrifuged at 100,000 *g* for 1 h. The pellets were suspended in buffer A and centrifuged again. The resultant pellets were suspended in buffer A containing various protease inhibitors, including 50 μM diisopropyl fluorophosphate (Wako), 50 μM phenylmethylsulfonyl fluoride (Sigma-Aldrich), 0.1 μg/ml N^{α}-*p*-tosyl-L-lysine chloromethyl ketone (Sigma-Aldrich), 0.1 μg/ml antipain (Peptide Institute), 0.1 μg/ml leupeptin (Peptide Institute), 100 μM EGTA (Wako), 1 mM thiorphan (Sigma-Aldrich), and 5 mM phenanthroline (Nacalai Tesque, Kyoto, Japan), for a final concentration of 2.5 mg protein/ml. The mixtures were incubated at 37°C for 1 h with CA-074, CA-074Me, or L-685,458. The reaction was terminated using a solution of chloroform:methanol (2:1). After extracting lipids with chloroform:methanol:water solution (1:2:0.8), the protein fractions were separated on conventional 16.5% Tris/Tricine gels to detect Aβ or AICD product by Western blot analysis.

In vitro degradation assay

In vitro cleavage of AICD was performed in 30 μl of 100 mM sodium acetate buffer (pH 5.5), containing 1 mM EDTA and 8 mM cysteine with or without synthetic AICD (Merck). Various amounts of purified cathepsin B from human liver (Merck) were added with or without 1 μM CA-074. The mixtures were incubated at 37°C for the indicated time, and sample buffer was then added to stop the reaction. The products were analyzed by Western blotting conventional 16.5% Tris/Tricine gels with an anti-APP antibody.

Statistical analysis

All values are expressed as means ± SE. For comparisons of 2 groups, a 2-tailed Student's *t* test was used. For comparisons among >3 groups, a Dunnett's or Student-Newman-Keul multiple comparison test was used. Differences were considered significant at values of $P < 0.05$.

RESULTS

Cathepsin B inhibitors, CA-074Me and E-64d, lead to the accumulation of CTFs and AICD with no change in α- and β-secretase activities

Weak bases, such as chloroquine or NH_4Cl, alkalize the intracellular pH of acidic compartments (19, 20). If there are proteases responsible for the degradation of CTFs and AICD other than γ-secretase, we should be able to detect the accumulation of CTFs by treatment with chloroquine or NH_4Cl in γ-secretase-deficient cells. To verify this hypothesis, we treated *PS1*$^{-/-}$ *PS2*$^{-/-}$ cells and APP_{NL}-H4 cells with chloroquine or NH_4Cl (**Fig. 1*A*, *B***). After chloroquine or NH_4Cl treatment, accumulation of CTFα was observed in *PS1*$^{-/-}$ *PS2*$^{-/-}$ cells (Fig. 1*A*). We were unable to detect CTFβ, which is derived from endogenous APP, likely due to the low β-secretase activity in these cells (Fig. 1*A*). In chloroquine- or NH_4Cl-treated APP_{NL}-H4 cells, we also observed accumulation of both CTFα and AICD with no change in FL-APP (Fig. 1*B*). Conversely, treatment with the γ-secretase inhibitor L-685,458 produced a significant accumulation of CTFs and lower production of AICD in APP_{NL}-H4 cells (Fig. 1*B*).

To address whether the cathepsin family is involved in degrading CTFs and AICD, we treated APP_{NL}-H4 cells with representative cathepsin inhibitors (Fig. 1*C*, *D*). Cathepsins B, D, and G are cysteine, aspartyl, and serine proteases, respectively. E-64d generally inhibits cysteine proteases. Western blot analysis showed that CTFα, CTFβ, and AICD did not significantly accumulate in the presence of inhibitors for cathepsins G and D (cathepsin G inhibitor I and pepstatin A, respectively), but E-64d and the cathepsin B-specific inhibitor CA-074Me markedly increased accumulation of CTFα, CTFβ, and AICD (Fig. 1*C*). In addition, treatment with the proteasome inhibitor lactacystin exerted no significant influence on the levels of CTFα, CTFβ, and AICD production (Fig. 1*C*). It has been reported that cathepsin B prefers wild-type APP (APP_{WT}) to APP_{NL} (12). Although CA-074Me treatment led to significant accumulation of CTFα, CTFβ, and AICD in stably APP_{WT}-overexpressing H4 cells (APP_{WT}-H4 cells), this efficacy in APP_{WT}-H4 cells was less than that observed in APP_{NL}-H4 cells (Supplemental Fig. S1).

If CA-074Me causes up-regulation of both α- and β-secretase activities, CTFα and CTFβ might simultaneously accumulate in cells. To evaluate the effects of CA-074Me on α- and β-secretase activities, sAPPα and sAPPβ levels were assessed in the conditioned medium from APP_{NL}-H4 cells treated with CA-074Me (Fig. 1*E*, *F*). No change in either sAPPα or sAPPβ levels was observed (Fig. 1*F*). Therefore, we concluded that cysteine protease cathepsin B was a major CTF- and AICD-degrading enzyme with no effect on α- and β-secretase activities.

Time course and dose dependency of the accumulation of CTFs and AICD *via* cathepsin B inhibition

To accurately assess the drug efficacy of CA-074Me, we performed time-course and dose-dependency analyses in APP_{NL}-H4 cells (**Fig. 2**). Time-course analysis revealed that CA-074Me treatment for 6 h or longer resulted in the gradual accumulation of CTFα, CTFβ, and AICD, as compared to 0 h of treatment (Fig. 2*A*, *B*). The effect of CA-074Me was observed to differ among CTFα, CTFβ, CTFs, and AICD. The accumulation of CTFα, CTFβ, and CTFs reached a peak at 12 h; in contrast, an accumulation of AICD showed a monotonic increase over a 0- to 24-h period (Fig. 2*A*, *B*). Dose-dependency analysis demonstrated that inhibition of cathepsin B by CA-074Me at 1 μM or more led to a significant accumulation of CTFα, CTFβ, CTFs, and AICD (Fig. 2*C*, *D*).

CA-074 and CA-074Me have no inhibitory effect on γ-secretase activity of the presenilin complex

Several drugs have been reported to inhibit or modulate γ-secretase activity, and nonsteroidal anti-inflammatory

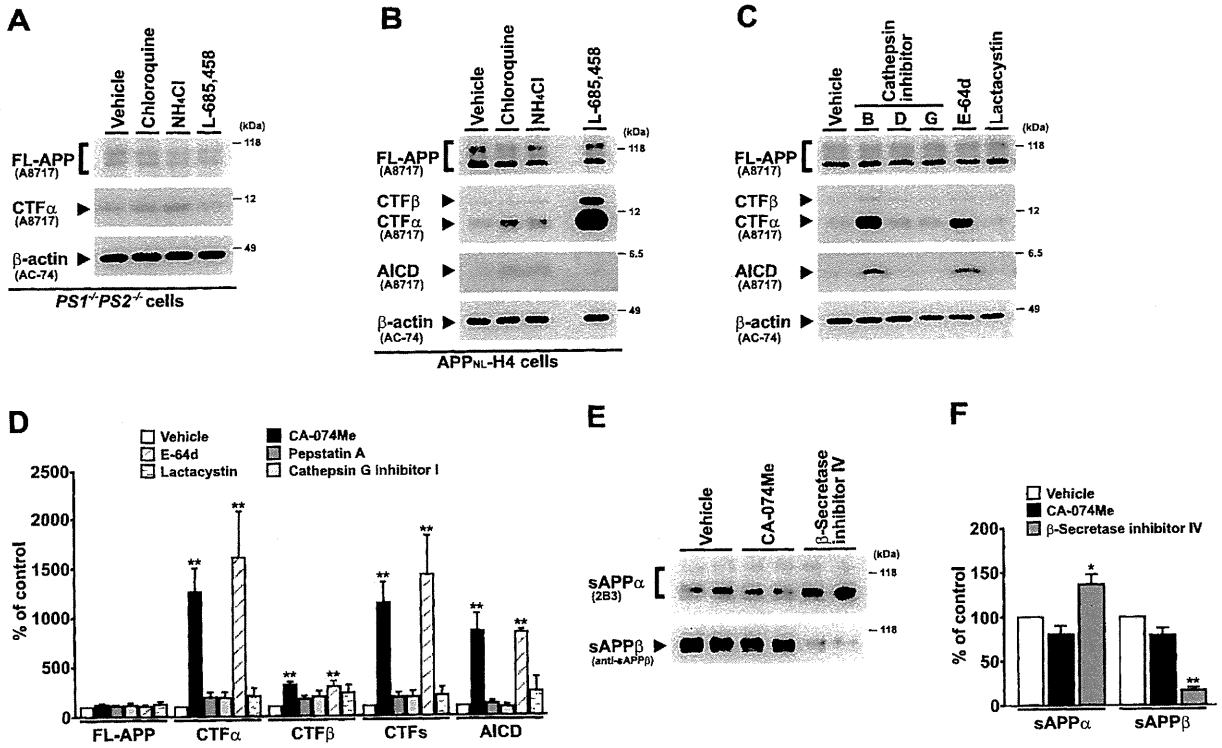

Figure 1. CA-074Me and E-64d lead to the accumulation of CTFs and AICD with no change in α- and β-secretase activities. *A*) Representative Western blots show the effect of treatment with chloroquine (1 μM), ammonium chloride (1 mM), or L-685,458 (1 μM) for 24 h on FL-APP, and CTFα levels in $PS1^{-/-}PS2^{-/-}$ cells. FL-APP and CTFα were detected with A8717; β-actin was detected with AC-74. *B*) Representative Western blots show the effect of treatment with chloroquine (1 μM), ammonium chloride (1 mM), or L-685,458 (1 μM) for 24 h on FL-APP, CTFα, CTFβ, and AICD levels in APP_{NL}-H4 cells. FL-APP, CTFα, CTFβ, and AICD were detected with A8717; β-actin was detected with AC-74. *C*) Amounts of FL-APP, CTFα, CTFβ, and AICD in the cell lysates of APP_{NL}-H4 cells treated with cathepsin inhibitors [B, CA-074Me (10 μM); D, pepstatin A (10 μM); G, cathepsin G inhibitor I (10 μM)], E-64d (10 μM), or lactacystin (1 μM) for 24 h were measured by semiquantitative Western blot analysis. β-Actin was used as loading control (*A–C*). *D*) Results of Western blot analysis shown in *C*. Data represent means ± SE of 5 experiments. $^{**}P < 0.01$: significantly different from the vehicle-treated group. *E*) Amounts of sAPPα or sAPPβ in conditioned medium from APP_{NL}-H4 cells treated with CA-074Me (10 μM) or β-secretase inhibitor IV (1 μM; as a positive control) for 24 h were measured by semiquantitative Western blot analysis with 2B3 or anti-sAPPβ antibody, respectively. *F*) Results of Western blot analysis shown in *E*. Data represent means ± SE of 4 experiments. $^{*}P < 0.05$, $^{**}P < 0.01$ *vs.* vehicle-treated group.

drugs (NSAIDs) are representative γ-secretase modulators that lower Aβ42 production and increase Aβ38 production. To elucidate the effects of CA-074Me on γ-secretase activity, we examined whether CA-074Me has a direct effect on γ-secretase activity (**Fig. 3**). We prepared a total cell membrane fraction of APP_{NL}-H4 cells and incubated this fraction with L-685,458, CA-074Me, or CA-074, which is a nonmethyl esterified analog of CA-074Me. Western blot analysis with anti-APP antibody showed that a γ-secretase inhibitor significantly suppressed production of AICD (Fig. 3*A*, lane 8; *B*). Treatment with cathepsin B-specific inhibitors CA-074 or CA-074Me did not suppress γ-secretase activity in the membrane fraction, as compared to treatment with vehicle (Fig. 3*A*, lane 3 *vs.* 4–7; *B*). Similarly, Western blot analysis with the antibody 82E1 showed that both CA-074 and CA-074Me failed to block production of Aβ (Fig. 3*C*, lane 3 *vs.* lanes 4–7, *D*). However, L-685,458 inhibited γ-secretase activity, leading to a decrease in Aβ levels, as compared to vehicle (Fig. 3*C*, lane 8; *D*). A weak band (Fig. 3*C*, lane 8) is believed to be Aβ preexisting in the membrane fraction (Fig. 3*C*, lane 2, bottom band of Aβ), and new Aβ was processed from longer Aβ (Fig. 3*C*, lane 2, top band of Aβ). This observation is consistent with a previous report that suggests longer Aβ can be processed to shorter Aβ by γ-secretase in the presence of L-685,458 without production of AICD (21). These results clearly demonstrate that the cathepsin B-specific inhibitors CA-074 and CA-074Me did not significantly affect the activity of γ-secretase.

Inhibition of cathepsin B has no inhibitory effect on Notch processing

With a rare exception, all γ-secretase substrates are membrane-associated stubs, which are type I membrane proteins with ectodomain shedding. The intracellular domain of several γ-secretase substrates cleaved by γ-secretase translocates into the nucleus, and this domain has been shown to activate transcription. To assess the effect of CA-074Me on the processing of Notch, another γ-secretase substrate, we treated $mNotch^{\Delta E}$-